Article

Patterns

EEG spectral attractors identify a geometric core of brain dynamics

Graphical abstract

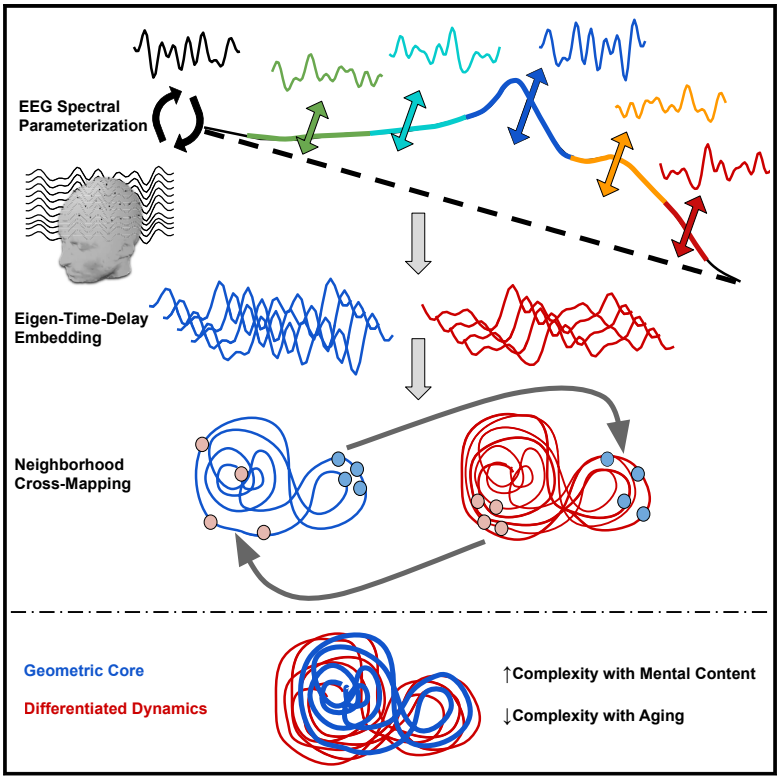

Authors

Parham Pourdavood, Michael Jacob

Correspondence

parham.pourdavood@ucsf.edu (P.P.), michael.jacob@ucsf.edu (M.J.)

In brief

Integration across parallel data streams is presumed to underlie the brain's information-processing capacity. How this is achieved from a kaleidoscope of signals is not understood. Adopting a data-driven, dynamical systems approach to ongoing brain rhythms, the authors examine the geometry of interactions between signals. This approach reveals shared global shapes that are embedded in the dynamics of brain signals. The complexity of mental content is hypothesized to differentiate out of this shared geometric core.

Highlights

- Geometry of EEG dynamics from multidimensional attractor reconstruction
- Low-complexity, core signatures predict frequency-band dynamics
- Low-complexity, homogeneous attractors in aging
- Thought content associated with more differentiated dynamics

Pourdavood & Jacob, 2024, Patterns 5, 101025
September 13, 2024 Published by Elsevier Inc.
https://doi.org/10.1016/j.patter.2024.101025

Patterns

CellPress
OPEN ACCESS

Article

EEG spectral attractors identify a geometric core of brain dynamics

Parham Pourdavood[1,2,*] and Michael Jacob[1,2,3,*]
[1]Mental Health Service, San Francisco VA Medical Center, 4150 Clement St., San Francisco, CA 94121, USA
[2]Department of Psychiatry and Weill Institute for Neurosciences, University of California, San Francisco, 505 Parnassus Avenue, San Francisco, CA 94143, USA
[3]Lead contact
*Correspondence: parham.pourdavood@ucsf.edu (P.P.), michael.jacob@ucsf.edu (M.J.)
https://doi.org/10.1016/j.patter.2024.101025

THE BIGGER PICTURE Brain signals display incessantly reverberating, rhythmic activity of high complexity. These signals interact in a linear and non-linear fashion to inform mental experience. From this interactive complexity, the brain is thought to contain a "dynamic core" that supports both the integration of information into a coherent whole and the differentiation of activity into phenomenal content. The neural substrates of this part-whole dynamic are unknown but could reflect a process-developmental hypothesis of brain activity, whereby the whole is sculpted to reveal the details. We examine this hypothesis geometrically, analyzing the evolving shape of brain signals in state space and causal asymmetries in their interactions with each other. Our findings support a process-developmental hypothesis: integrative dynamics are shared across frequency bands, co-occurring with more complex, differentiated dynamics and with a loss of this differentiated complexity in older adults.

SUMMARY

Multidimensional reconstruction of brain attractors from electroencephalography (EEG) data enables the analysis of geometric complexity and interactions between signals in state space. Utilizing resting-state data from young and older adults, we characterize periodic (traditional frequency bands) and aperiodic (broadband exponent) attractors according to their geometric complexity and shared dynamical signatures, which we refer to as a geometric cross-parameter coupling. Alpha and aperiodic attractors are the least complex, and their global shapes are shared among all other frequency bands, affording alpha and aperiodic greater predictive power. Older adults show lower geometric complexity but greater coupling, resulting from dedifferentiation of gamma activity. The form and content of resting-state thoughts were further associated with the complexity of attractor dynamics. These findings support a process-developmental perspective on the brain's dynamic core, whereby more complex information differentiates out of an integrative and global geometric core.

INTRODUCTION

Since their discovery, electrophysiologic signals have been defined by rhythmicity. This has led to a "rhythms of the brain" approach to studying physiologic processes by linking putative cognitive functions to indices of frequency-based activity, such as power and phase coherence.[1] This approach has been expanded by growing evidence that interactions between frequency bands, so-called cross-frequency coupling, underlie cognitive function,[2–5] and that disruptions in synchronized activity contribute to neuropsychiatric dysfunction.[6,7] Cross-frequency interactions are characterized by pairwise measures of coherence and/or correlation, often interpreted as connectivity, since they are thought to reflect functional interactions between local or global brain networks, depending on the frequency bands involved.[8,9] Analytic pitfalls notwithstanding,[10] these approaches generally emphasize linear assessment of time-frequency decomposition linked to a stimulus or task. Emerging evidence for the importance of aperiodic activity (not defined by a distinct frequency) complicates analysis of cross-frequency interactions,[11–14] raising the necessity of identifying new methods to investigate interactions between aperiodic and periodic parameters.

In parallel with these developments in the study of brain rhythms, alternative perspectives have examined brain activity as a multidimensional signal, with complex, non-linear, and non-stationary

dynamics.[15–17] Although signal complexity of this nature is often dismissed as random variance, it may contribute meaningfully to cognition and behavior as part of a globally integrated, dynamical system.[18,19] One approach to analytically utilize this dynamical systems perspective is to embed physiologic signals onto a multidimensional state-space manifold.[15,20–22] When manifold dynamics converge, this suggests that the system may be operating as an attractor.[15] The multidimensional geometry of interacting attractor systems can yield highly relevant information on causality across a wide range of applications, known as Sugihara causality, or convergent cross-mapping (CCM).[23,24] Complementary to information theoretical methods that can also handle non-linear EEG data,[25–28] cross-mapping approaches are model-free and geometric rather than statistical and probabilistic (such as transfer entropy). Since geometric approaches do not rely on digitization or quantization of the underlying signal, they may be better suited to complex high-dimensional systems, where the continuous dynamics must be preserved.[29–31] Related methods have ushered in a "geometric approach" to analyzing the dynamic signatures and motifs of brain activity in state space, which could help make sense of what neural signals represent.[32–34] Although state-space embedding procedures have long been used to investigate EEG activity,[20,22] such approaches are not typically employed to investigate cross-parameter coupling. Manifold-to-manifold or attractor-to-attractor geometric mapping relationships are necessary to determine dynamical systems interactions within the structure of EEG itself and especially where traditional cross-frequency coupling approaches may not be appropriate.

Geometric approaches have helped identify regional dynamics from fMRI that are common across a range of cognitive tasks.[35] These shared dynamics cut across traditional functional networks and are based instead on unique, topological signatures in the dynamics of activity. The resulting regions and their dynamical manifolds have been reported as evidence of an integrative "dynamic core" in the brain. The concept of an integrative core was originally attributed to Varela,[36] who proposed that specific cognitive operations reflect transient synchronization that emerges from ongoing activity in a dynamically unstable dominant assembly.[36,37] Varela emphasized the wholeness of living systems, with parts undergoing transformation to support self-regeneration of the whole.[38] His theoretical work contributed to a process-developmental view of cognition (microgenesis), analogous to embryogenesis, whereby complex mental states differentiate out of a global core of putatively brainstem-driven activity.[39,40] Like transformations in embryological form (morphogenesis), this view of cognition is conceptually geometric, but little empirical work has been devoted to the topic.

The term "dynamic core" was used by early gestalt psychologists[41] and later adopted by Tononi and Edelman to capture a continually varying, unified process that yields high degrees of integration, differentiation, and complexity.[42] Their hypothesis was based on considering integration with respect to synchronization in the rhythmic activity of the brain and differentiation (neural complexity) in information-theoretic terms. The complexity of neural activity has long been linked to the level, state, and content of consciousness[43,44]; however, purely information-theoretic measures might conflate levels of consciousness (e.g., degree of arousal) with the content of consciousness (e.g., thoughts, sensations, emotions).[45,46] Therefore, the concept of a dynamic core can be re-examined in light of contributions from arrhythmic (aperiodic) activity that is linked to changes in arousal[47–49] and geometric perspectives that could relate process-developmental theories to computational work on the neural representation of mental states.[34,50]

Cognitive aging provides an exemplar case of changes in the aperiodic and periodic composition, in part linked to the hypothesized loss of complexity[51–53] and loss of signal differentiation in aging.[54–57] A "redundancy core" has been hypothesized for older adults, a putative link between dynamic core models, the loss of complexity, and loss of differentiation.[58] Recent studies of aperiodic EEG in cognitive aging are generally consistent with a loss of complexity,[59–61] reporting a flatter spectra (lower aperiodic exponent) that has been interpreted as increased neural noise[62] and/or a loss of long-range temporal correlations that may help coordinate behavior and cognition across multiple scales.[5,63] Therefore, the geometry of ongoing aperiodic and periodic activity, as measures of a putative electrophysiologic dynamic core, provide a highly relevant framework to examine complexity and signal differentiation in aging.

Given the promise of geometric, manifold-based representations of neural data, we reasoned that the dynamic core of EEG might be evident in shared dynamics across the frequency domain. To define the geometry and ascertain the complexity of EEG spectral dynamics, we used state-space embedding procedures and a CCM-based measure of geometric cross-parameter coupling during a resting-state paradigm. We hypothesized a loss of geometric complexity in older adults that would correlate with greater shared dynamics between EEG parameters, yielding a less differentiated dynamic core. Across all participants we find that the dynamics of the alpha band and the aperiodic exponent contain a low-dimensional core set of dynamically unstable, geometric signatures that predict the dynamics of other EEG parameters. As hypothesized, older adults show reductions in the geometric complexity of ongoing periodic and aperiodic signals that are linked to more homogeneous core dynamics. We further examined associations between geometric complexity and the form and content of resting-state thoughts. Our findings emphasize the inherently unstable nature of the EEG's dynamic core, whereby higher-frequency operations differentiate out of core dynamics to yield structures of higher complexity. This work has implications for dynamical systems theories of neural function and models of aging.

RESULTS

Aperiodic and periodic EEG parameters

EEG parameterization enables decomposition of an electrophysiologic signal into periodic (oscillatory) activity that appears to rise above an aperiodic (arrhythmic) and scale-free background.[12] Although the underlying generators of aperiodic activity remains unknown,[64,65] this activity is thought to reflect excitability across neural networks[66,67] and coordination across multiple temporal scales,[68,69] and to be linked to a wide range of cognitive processes[70,71] and pathologies.[72] Since aperiodic and periodic signals are ongoing at rest and both likely contribute to the dynamic core of resting brain activity, we first parameterized our EEG spectra to examine group differences in average periodic and aperiodic activity (Figures 1A and 1B). As expected, older adults

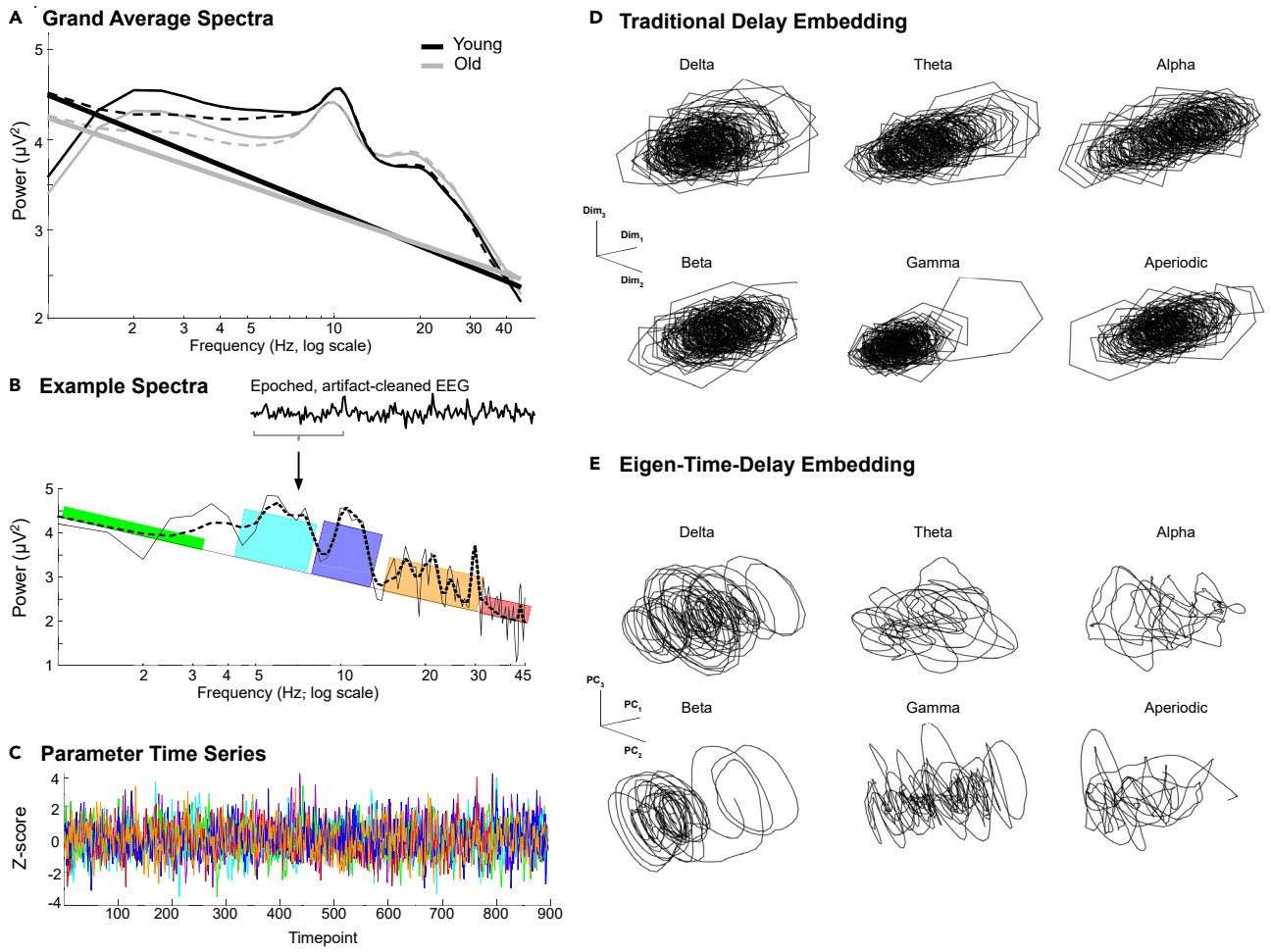

Figure 1. EEG parameterization and embedding methods

(A) Average spectra from the subset of channels utilized for this study during eyes closed (EC) for young adult (YA; $n = 138$, black) and older adult (OA; $n = 63$, gray) participants. Dashed line indicates full FOOOF model fit, and the solid, thick line indicates the aperiodic fit.

(B) An example of extracted EEG parameters using FOOOF for one epoch, from one participant; light green (delta), cyan (theta), blue (alpha), yellow (beta), and red (gamma).

(C) Normalized time series for each parameter in the same colors from the participant in (B).

(D) Each parameter's time series is used to reconstruct its high-dimensional attractor using traditional time-delay embedding.

(E) Eigen-time-delay attractors are plotted from the first three principal components (PC1, PC2, PC3).

(OAs) show a smaller aperiodic exponent, yielding a flatter aperiodic slope, compared with young adults (YAs), which was most pronounced during the eyes-open (EO) condition (AGE × CONDITION $F(1,199) = 25.55$, $p < 0.00001$; OAs: $\text{exponent}_{EC} = 0.98$, $\text{exponent}_{EO} = 0.83$ and YAs: $\text{exponent}_{EC} = 1.15$, $\text{exponent}_{EO} = 1.10$). For residual periodic power, we found a significant AGE × CONDITION interaction effect ($F(5,995) = 7.01$, $p = 0.002$). This was attributable to OAs showing less residual power in the theta and alpha bands (Tukey's honest significant difference [THSD], all corrected p values <0.05), more residual power in the beta range (THSD p values <0.00001), and more residual power in the gamma range in the EO condition only (THSD $p = 0.04$).

Spectral attractor complexity

Variability in ongoing physiologic dynamics provides additional complexity that is thought to underpin fluctuations in cognition and behavior.[18,19] We reasoned that ongoing variability and complexity in periodic and aperiodic signals could be examined from multidimensional embedding of signal dynamics. To assay complexity, we utilized an embedding procedure known as eigen-time-delay (ETD) embedding that orders manifold dynamics as principal components (dimensions) from an intermittently forced linear approximation.[73] That is, ETD embedding yields multidimensional manifolds that capture the trajectory of an EEG parameter's dynamics over the course of a resting-state scan and that might be influenced by state (eyes open or closed) or age. We used the number of significantly retained components (dimensions) as a measure of geometric complexity for each parameter and participant.

Each parameter revealed idiosyncratic trajectories, although there appeared to be globally regular dynamics, suggestive of

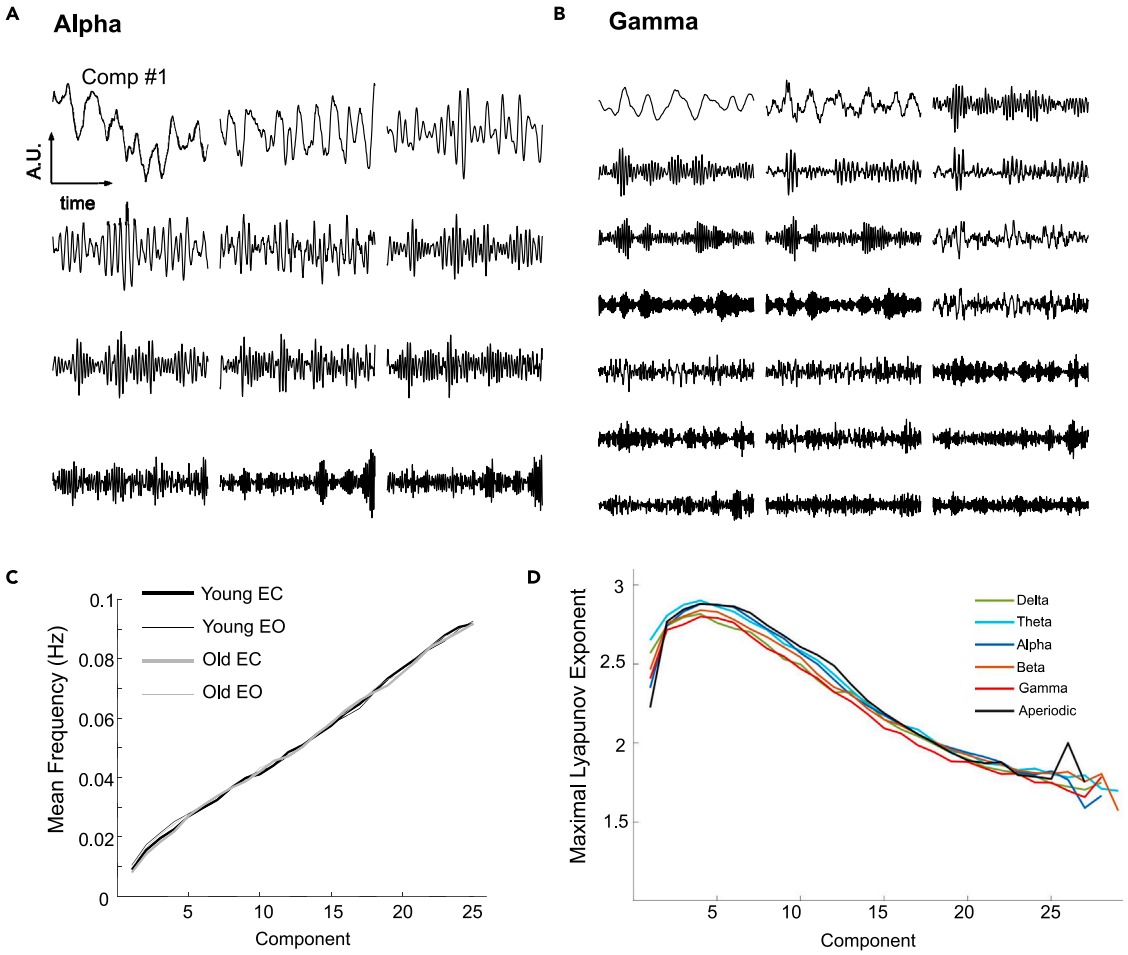

Figure 2. Eigen-component dynamics

(A and B) The first 12 principal components of alpha (A) and 21 components for gamma (B) for one participant. Components are ordered from left to right, ranked by the magnitude of the component eigenvalue.

(C) Mean frequency of components (ordinate) plotted against the component number (abscissa) and averaged across all EEG parameters for YA (black) and OA (gray) participants during the EC (thick lines) and eyes-open (EO) (thin line) conditions.

(D) Maximal Lyapunov exponent (MLE, ordinate) plotted against the component number (abscissa) and averaged across EC and EO conditions for delta (green), theta (cyan), alpha (blue), beta (orange), gamma (red), and aperiodic (black).

complex attractor manifolds (Figures 1D and 1E). Examining the ETD components individually reveals repetitive, rhythmic dynamics of increasing mean frequency and ranging from 0.01 to 0.1 Hz (Figures 2A–2C). This monotonic relationship between increasing mean frequency and component number (main effect of COMPONENT: $F(1,3705) = 245.22$, $p < 0.00001$) did not depend on condition ($p = 0.99$) or age ($p = 0.62$), with a slight reduction (absolute difference ~0.0002 Hz) in the aperiodic exponent and no differences between all other frequency bands (main effect of PARAMETER $F(1,3705) = 5.95$, $p < 0.00001$ and no interaction effects, all p values <0.13). We also characterized the ETD components by their maximal Lyapunov exponent (MLE, Figure 2D), which provides a statistical measure of the stability of the underlying dynamics, that is, whether the dynamical trajectory is converging, diverging, or stable. We found a positive MLE across all components, suggestive of unstable dynamics, with the maximum exponent present at components 3 or 4 (main effect of COMPONENT: $F(1,3705) = 170.4$, $p < 0.00001$, Figure 2D). MLE did not depend on condition ($p = 0.99$) or age ($p = 0.76$) and showed only subtle differences between EEG parameters across dimension (Figure 2D, PARAMETER × COMPONENT $F(1,3705) = 1.53$, $p < 0.0008$ and no other interaction effects, all p values <0.4).

Thus, despite qualitatively idiosyncratic attractor trajectories, all EEG parameters for all conditions and groups showed similarly unstable rhythmic dynamics. Nonetheless, the percent variance explained by each ETD component was different for each parameter, condition, and group. For YA participants, the first component of alpha during the eyes-closed (EC) condition captured the most variance (~15%). By contrast, for OA participants, the first component of the aperiodic parameter in the EC condition captured the most variance (~18%; see Figure 3). These differences in the distribution of explained variance resulted in differences in attractor complexity between parameters, conditions, and groups (based

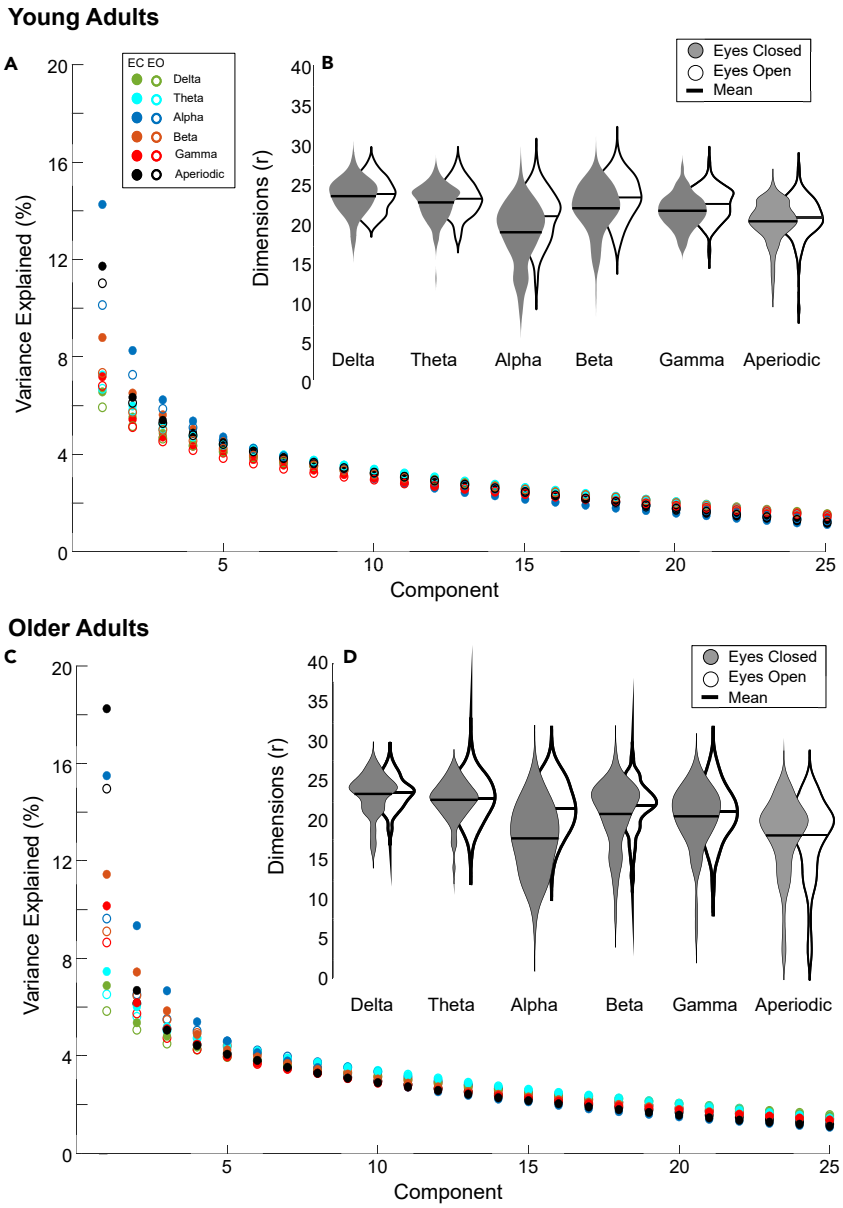

Figure 3. Parameter variance and geometric complexity

The average percentage of variance explained by each of the first 25 principal components (abscissa) across YA participants (A) and OA participants (C) for delta (green), theta (cyan), alpha (blue), beta (orange), gamma (red), and aperiodic (black), for eyes closed (filled circles) and eyes open (open circles). Violin plots display a Gaussian smoothed distribution estimate of attractor dimensionality (geometric complexity) for each EEG parameter across YA (B) and OA (D) participants for EC (gray) and EO (white) conditions, with the mean complexity score indicated by the horizontal lines.

on the number of statistically significant retained components, see experimental procedures). All participants showed increased complexity during EO for periodic parameters (main effect of CONDITION, $F(5,995) = 63.6$, $p < 0.0001$) and the aperiodic exponent (main effect of CONDITION, $F(1,199) = 8.75$, $p < 0.005$). We found that the alpha attractors are the least complex relative to all other periodic parameters (main effect of PARAMETER, $F(5,995) = 17{,}804$, $p < 0.0001$). OA participants showed lower attractor complexity (main effect of AGE, $F(1,199) = 5.63$, $p < 0.05$ and AGE × CONDITION × PARAMETER, $F(5, 995) = 2.47$, $p < 0.05$) in the beta and gamma attractors during the EO condition (THSD corrected $p < 0.005$) and gamma attractors in the EC condition (THSD corrected $p < 0.05$). OAs similarly showed lower complexity in their aperiodic attractors across conditions (main effect of AGE, $F(1, 199) = 13.30$, $p < 0.0005$ without AGE × CONDITION effects).

In general, we found modest or no association between the magnitude of residual periodic power and attractor geometric complexity. When controlling for group and condition, greater alpha power modestly predicted less geometric complexity (partial $r = -0.37$, $p < 0.0005$) with subtle, but significant differences in this association between young and old participants ($r_{Young} = -0.27$, $p_{Young} < 0.005$ and $r_{Old} = -0.3$, $p_{Old} < 0.05$; AGE × POWER interaction t-statistic = 5.07; $p < 0.0001$). There was no significant association between delta, theta, or beta power and corresponding geometric complexity (delta: $r = 0.02$, $p = 0.73$; theta: $r = -0.05$, $p = 0.34$; beta: partial $r = -0.06$, $p = 0.20$) and no significant differences in the association between groups (all p values >0.05). Only gamma attractors in young participants revealed significant associations between power and geometric complexity (YAs: partial $r = 0.23$, $p = 0.006$; OAs: partial $r = -0.20$, $p = 0.12$; AGE × POWER t-statistic = 1.99, $p = 0.047$). For aperiodic attractors, a larger aperiodic exponent was minimally correlated with greater complexity (partial $r = 0.16$, $p = 0.001$; without differences between groups, $p = 0.18$). Thus, the geometric complexity of spectral attractors is not simply a reflection of the mean power or mean aperiodic exponent and reflects unique dynamical signatures.

Geometric cross-parameter coupling

The above evidence for differences in the geometric complexity of EEG parameters and for differences in complexity between old and young participants motivated the examination of shared dynamics from geometric reconstructions. Based on the dynamic core model of brain function, we reasoned that less complex parameters would be more integrative, and thus contain the simple dynamics that are shared across parameters. By contrast, more complex parameters would be more differentiated and specialized, that is, less integrative and with less shared dynamics across parameters. To examine the magnitude of geometric cross-parameter coupling between spectral attractors,

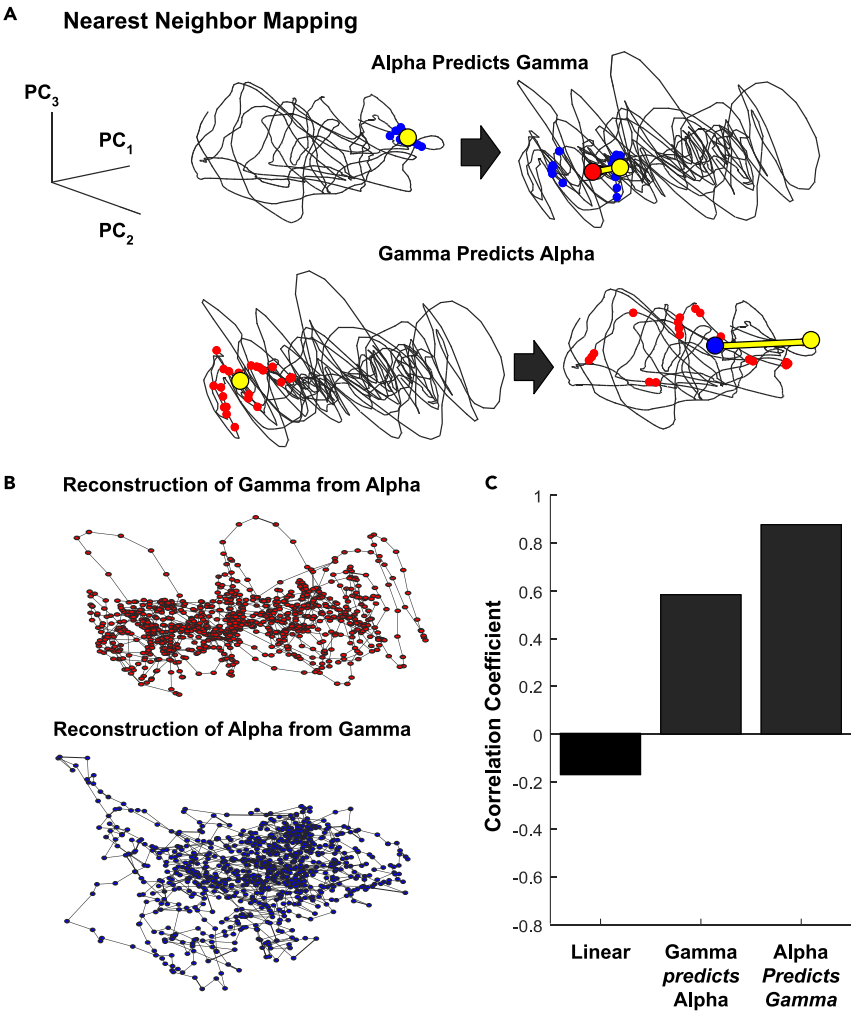

Figure 4. Geometric cross-parameter coupling methods

(A and B) (A) An example of geometric cross-parameter coupling for a single participant. Top row, alpha predicts gamma: A random point (large yellow circle) on alpha's attractor and its nearest neighbors (small blue circles) are mapped onto gamma's attractor via the timestamps of the neighbors on the alpha manifold (also designated by yellow and blue circles). The distance-weighted average of the mapped neighbors is designated by the large red circle, and the total set of these averages is used to reconstruct a predicted gamma manifold by alpha (shown in B). The distance between the actual point on gamma (yellow circle) and the alpha's prediction (red circle) is given by the thick yellow line; this distance is less than the corresponding prediction of alpha by gamma (see bottom row). Bottom row, gamma predicts alpha: Utilizes the same convention as above.

(C) Bar plot of the magnitude of the correlation coefficients between alpha and gamma time series (left), between the original alpha manifold and gamma's manifold prediction of alpha (middle), and between the original gamma manifold and alpha's manifold prediction of gamma (right).

we used eigen manifold cross-mapping (EMCM) to measure shared non-linear dynamics between parameters on a participant-by-participant basis (Figure 4). EMCM (and CCM more generally) generates a predicted attractor based on a nearest-neighbor approximation that is then correlated with the other parameter's attractor. Thus, EMCM provides a measurement of shared shape between dynamics, which we refer to as geometric cross-parameter coupling.

To quantify the degree of geometric cross-parameter coupling, we report EMCM scores, which are the eigen-weighted average of all pairwise predictions between ETD dimensions. In general, we find moderate to high geometric coupling across all parameters, that is, most spectral attractors can predict the dynamics of the others (mean EMCM score of 0.56, range 0.26–0.99 across all participants and conditions). As described in the experimental procedures and unlike linear correlation (which yields a singular statistic, Pearson's r for the pairwise relationship), EMCM yields two output statistics: one indicating the strength of prediction when signal a is the "predictor" and signal b "predicted" (a predicts b) and another when the signals are reversed and parameter b is the "predictor" and parameter a is "predicted" (b predicts a) Therefore, unlike a symmetrical linear connectivity matrix (see supplemental information), the top and bottom of the EMCM matrix are non-identical (Figure 6). If we assume that each parameter contains a dynamical signature of the core, an asymmetry might arise if one parameter is more integrative than the other.

To illustrate an example of asymmetry in shared dynamics between parameters, we selected an exemplary participant and parameter-parameter coupling to display (alpha to gamma and gamma to alpha, Figures 4, 5A, and 5B). We found that the highest correlations between "predictor" dynamics and the "predicted" dynamics were for the lower dimensions of the manifold, typically the first 15 dimensions that account for ~56%–65% of the variance, not only for this example participant but across all participants, parameters, and conditions (Figures 5C–5F). This finding suggests that a relatively low-dimensional set of core dynamics are shared across all EEG spectral parameters.

Across conditions, and in YAs and OAs alike, alpha predicted all other spectral attractors the best, particularly in the EC condition (PARAMETER × CONDITION, $F(1,5,771) = 14.07$, $p < 0.0001$; Figures 6C and 6D, vertical yellow bands, THSD for all alpha EC prediction p values <0.0001). In geometric terms, this means that the alpha attractor contains signatures that are the most shared among all other attractors (i.e., alpha has the most generic dynamical signatures). The aperiodic exponent exhibits a similar pattern, whereby most other parameters show greater EMCM scores when they are predicted by the aperiodic parameter (THSD for all aperiodic EC prediction p values (except alpha) <0.0001). OAs show greater EMCM scores across conditions (main effect of AGE, $F(1,5,771) = 6.61$, $p = 0.010$). This is most

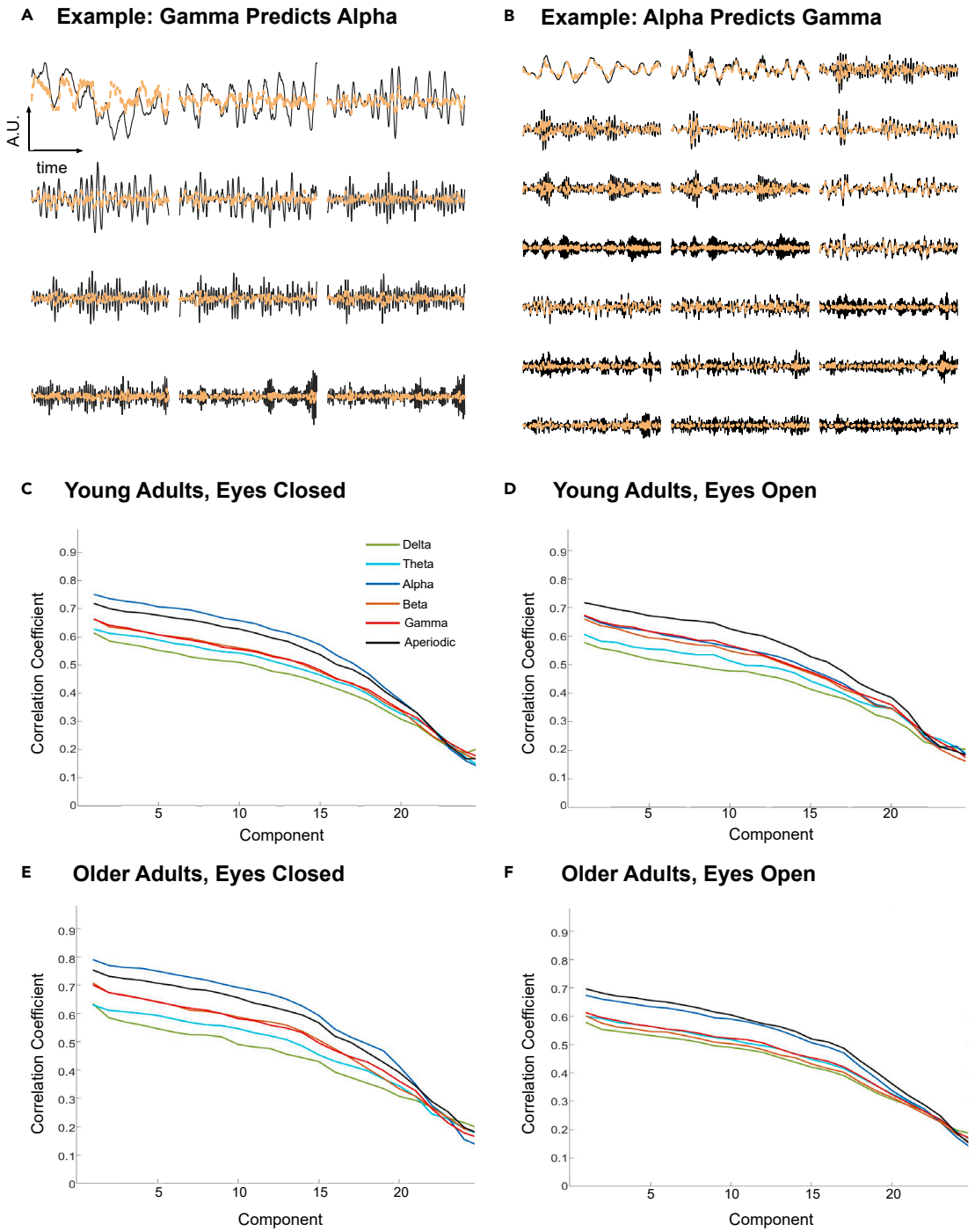

Figure 5. Lower-dimensional dynamics are most predictive

(A) The dynamics of the first 14 principal components of alpha and their prediction by nearest neighbors of gamma's manifold (dashed orange) for one participant.
(B) The dynamics of the first 21 principal components of gamma and their prediction by nearest neighbors of alpha's manifold (dashed orange) for one participant.
(C–F) Average prediction scores for each component by EEG parameter for YAs during EC (C) and EO (D) conditions and for OAs during EC (E) and EO (F) conditions.

pronounced when the higher-frequency attractors and the aperiodic exponent are predictors (AGE × CONDITION × PARAMETER, $F(1,5,771) = 2.63$, $p < 0.0001$; significance of follow-up tests using THSD are shown in Figure 6).

In general, we find that EEG attractors with reduced dynamical complexity are better predictors, that is, their dynamics are most similar to the set of low-dimensional, core-like dynamics of more complex attractors. This was true across all participants and

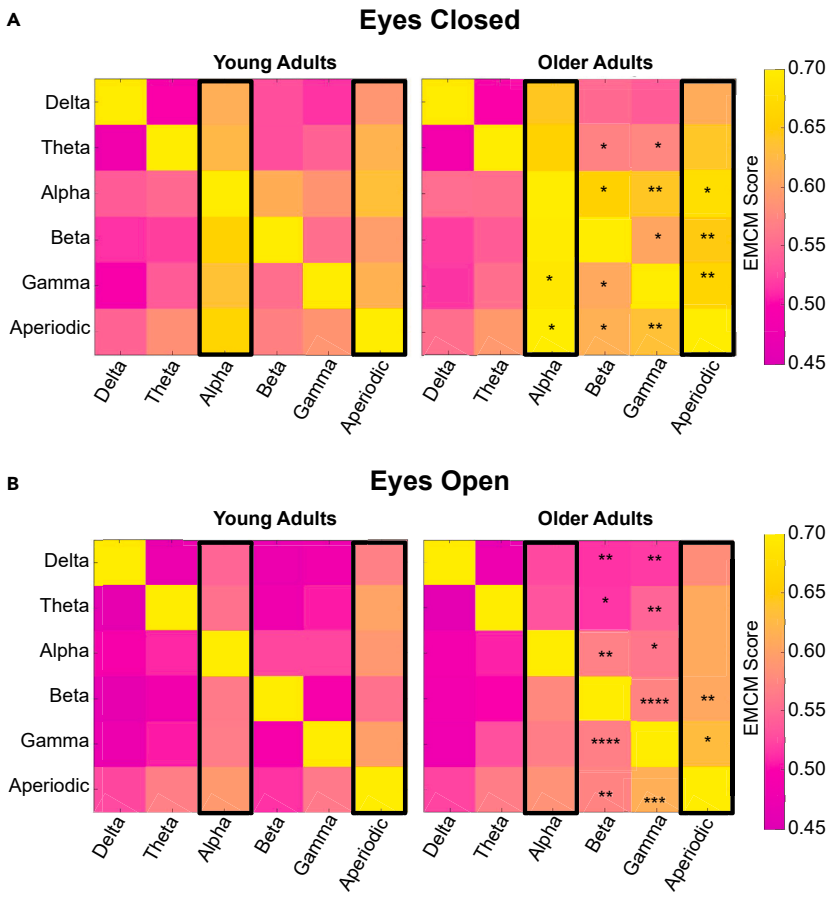

Figure 6. Geometric cross-parameter coupling by condition and group

EMCM matrices for all parameters (delta, theta, alpha, beta, gamma, aperiodic); the magnitude of the EMCM score is given by the color bar for YAs (left) and OAs (right) in EC (A) and EO (B) conditions. Significant differences are indicated by asterisks. Boxes denote parameters with core-like, shared dynamics. The asterisks signify the Tukey's honestly significant differences between YA and OA participants (*$p < 0.05$, **$p < 0.005$, ***$p < 0.0005$, ****$p < 0.00005$).

conditions. Alpha attractor complexity is inversely correlated with EMCM scores across parameters while controlling for age and condition (all partial r values <-0.86 and all p values <0.0001, and no AGE × CONDITION effects). In contrast, the geometric complexity of the other parameters was only modestly associated with lower EMCM scores (delta complexity $r = -0.46$, theta $r = -0.37$, beta $r = -0.56$, gamma $r = -0.45$, exponent $= -0.42$, all p values <0.0001). Similar to alpha, aperiodic attractor complexity inversely correlated with EMCM scores (all partial r values <-0.79 and all p values <0.0001, no AGE × CONDITION effects) and where dynamical complexity of the other bands only modestly predicted lower EMCM scores (delta $r = -0.50$, theta $r = -0.54$, alpha $r = -0.52$, beta $r = -0.60$, gamma complexity $r = -0.58$, all p values <0.0001). These correlations are entirely eliminated if the complexity of the opposite condition attractor is used (e.g., the complexity of the EO alpha attractor cannot predict the EMCM scores of EC delta, theta, beta, and gamma). This suggests that the correlation between complexity and prediction scores depends on the unique condition-dependent geometric structure of the spectral attractors.

Correlations with resting-state thoughts

Similar to others, we hypothesized that the geometric complexity of EEG attractors might be associated with participants' mental state at rest.[43,44] To explore this possibility, we utilized responses to the New York Cognition Questionnaire collected from an fMRI session the day before the EEG session. We reasoned that the form and content of mental activity at rest would be habitual, automatic, and recurring,[74–76] and well captured by the attractor paradigm.[77] Thus, although we do not have access to the form and/or content of the participants' mental state during the EEG recording, we hypothesized that there might be some similarity between the resting mental state during EEG and fMRI sessions. Following Gorgolewski et al., we used factor analysis to identify dimensions of content and form, yielding similar factor-loading matrices.[78]

OA participants showed lower factor scores related to thoughts about the past or future ($t = 3.30$, $p = 0.001$, $t = 5.35$; $p < 0.001$) as well as lower factor scores about positive thoughts ($t = 2.96$, $p = 0.003$) but not negative thoughts ($t = 1.23$, $p = 0.21$). OAs showed higher factor scores related to thoughts about friends ($t = -3.32$, $p = 0.001$). Regarding form, OAs showed lower factor scores related to imagery ($t = 5.04$, $p < 0.0001$) and vagueness ($t = 5.58$, $p < 0.0001$) but not verbal thoughts ($t = 0.96$, $p = 0.34$). Given the exploratory nature of this analysis, we included the complexity of all EEG parameters as predictors of form and content in repeated-measures, multiple linear regression analysis that included age and condition as covariates. After controlling for multiple comparisons, only the complexity of gamma-band attractors was associated with factor scores for negative thoughts ($p_{FDR} = 0.016$, partial $r_{Young} = 0.21$, $r_{Old} = 0.17$) without differences in the magnitude of this correlation between groups ($p = 0.11$). Except for aperiodic attractor complexity, there were no interaction effects between parameter complexity and age in predicting mental state. For OAs (but not YAs) the complexity of the aperiodic attractor correlates with the factor scores for positive thought content (partial $r_{Young} = -0.12$, $r_{Old} = 0.25$, AGE × COMPLEXITY $p_{FDR} = 0.017$) and visual imagery (partial $r_{Young} = -0.11$, $r_{Old} = 0.31$, AGE × COMPLEXITY $p_{FDR} = 0.017$).

DISCUSSION

In summary, we have implemented ETD embedding to characterize the geometric complexity of EEG spectral dynamics. This approach examines an EEG parameter's signal embedded in state space and uses principal component analysis to determine the minimum number of components (dimensions)

necessary to capture those dynamics. The output of this approach yields attractors that describe the "shape" of an EEG parameter's dynamics. The local geometry of this shape is characterized by the Lyapunov exponent (instability) and the extent to which local neighborhoods can predict the location of neighborhoods on another parameter's manifold, which we refer to as geometric cross-parameter coupling. These analyses reveal that the two hallmarks of ongoing activity in the resting EEG spectra, alpha power and the aperiodic exponent, contain generic geometric signatures that are shared among all other parameters.

Following the terminology of Shine et al.,[35] we refer to these parameters as "core," since the principal components of alpha and aperiodic dynamics are geometrically represented across other frequency bands (analogous to the dynamics of specific brain networks being represented across multiple tasks in Shine et al.). Our "core" designation is consistent with Varela's unstable, dominant assembly,[36,37] and his notion of eigenbehaviors, which reflect preferential recurrence within neurobehavioral state space (and is consistent with our extraction of dynamical principal components).[38,79] However, our core differs from the concept of Tononi and Edelman[42] in the sense that our approach evaluates complexity in geometric rather than information-theoretic terms. Low-dimensional core dynamics are embedded in parameters with higher geometric complexity (delta, theta, beta, and gamma), suggesting that EEG spectral dynamics reflect a spectrum from more integrative (alpha/aperiodic) to more differentiated. Next, we interpret these findings in the context of dynamical systems theory, geometric interpretations of neural data, and theories of cognitive aging.

Geometric attractor complexity

Although there is a long history of applying state-space embedding methods to EEG analysis,[20,22] geometric analyses of manifolds have only recently been applied, and generally to the dynamics of the whole EEG or electrocorticography (ECoG) spectrum.[80–82] However, EEG dynamics reflect a mixture of periodic signals across a range of frequency bands in addition to contributions from aperiodic components, sometimes referred to as scale-free because this activity lacks a dominant temporal frequency. Therefore, rather than representing a singular statistic for the entire EEG, complexity scores may vary from parameter to parameter, which informed the approach we took here. Critically, we found that alpha and aperiodic parameters are the least complex whereas low- and high-frequency activity (on either side of the alpha peak) showed greater geometric complexity. This is consistent with a widely employed heuristic that a shift toward higher-frequency activity is indicative of brain activation,[83] as gamma-band power has been studied extensively in relation to cognitive tasks[84,85] and as a putative marker of E/I balance in resting-state studies.[86] Thus, our finding of increased complexity in the beta and gamma bands is consistent with these bands' putative role in more complex cognitive tasks. Further, that gamma complexity was the only parameter associated with thought content during the resting-state task is consistent with evidence linking gamma-band activity to ruminative thinking (negative recurring patterns of thought).[87] If the resting state represents a diverse sampling of states of mind,[78,88] then we speculate that participants with greater gamma complexity may have been more engaged with ruminative thinking. This hypothesis is supported by a shift toward lower-frequency activity during states of mindfulness, a period of reduced ruminative mental activity.[89]

Geometric cross-parameter coupling

Our use of geometric complexity enabled a novel analysis of cross-parameter coupling based on the geometry of local dynamics for each EEG parameter. Whereas linear correlation found modest relationships between nearby EEG parameters (most notably alpha and beta), the geometric approach we utilized found that alpha and aperiodic signals showed the most robust coupling between other EEG parameters. Cross-parameter (typically cross-frequency coupling) is a well-established analytical approach to task-based brain-cognition-behavior relationships.[2–5] A related concept of intrinsic coupling has been advanced to examine resting or ongoing brain activity that considers either band-limited phase coupling or coupling in the envelope (amplitude) of signal fluctuations.[90] Our application of geometric cross-parameter coupling adopts the latter approach, embedding the signal envelope of EEG parameters into state space. This enables us to examine potential interactions across a range of periodic and aperiodic signals. More importantly, it allowed us to examine non-linear and directed interactions between neural signals from cross-mapping methods.[91]

CCM was developed by Sugihara and colleagues to infer directed-causal interactions between highly non-linear signals.[23,24] Subsequently, CCM has been applied to ECoG recordings in non-human primates,[91] multielectrode recordings in rats,[92] and to a limited extent in human EEG.[93–95] Similar to Tajima et al.,[91] we found a high degree of bidirectional interaction between neural signals that would be otherwise missed from purely linear approaches. Alpha and aperiodic parameters stood out in their ability to predict the non-linear dynamics of all other frequency bands. In the language of Sugihara causality, this means that all other frequency bands have molded the dynamics of these core bands (i.e., caused their dynamics). As a result of being involved in more processes, alpha and aperiodic signals ended up with the most generic and accommodating dynamics that are the least complex. This perspective is broadly consistent with contributions of alpha and aperiodic signals to general arousal[48,96–98] and alpha's role as a brain-wide inhibitory signal across task and resting states.[99]

Neurobiology of the dynamic core

We have utilized a geometric perspective to investigate a seeming paradox of the dynamic core hypothesis: that neural activity is simultaneously capable of integration (unification or binding across diverse subsystems) and differentiation (access to a large repertoire of dynamical states). By considering core dynamics across frequency bands, we find that integrative dynamics are embedded in more complex (differentiated) dynamics. That is, we use geometric methods to examine temporal dynamics in a spatial manner ("time is neuronal space in the brain").[1] This establishes an asymmetry within core dynamics such that aperiodic, and particularly alpha, represents a geometric core of activity that predicts all other frequency bands. This finding is highly consistent with the hypothesis of a thalamic core of brain function,[100,101] based on the prevailing view that alpha signals reflect

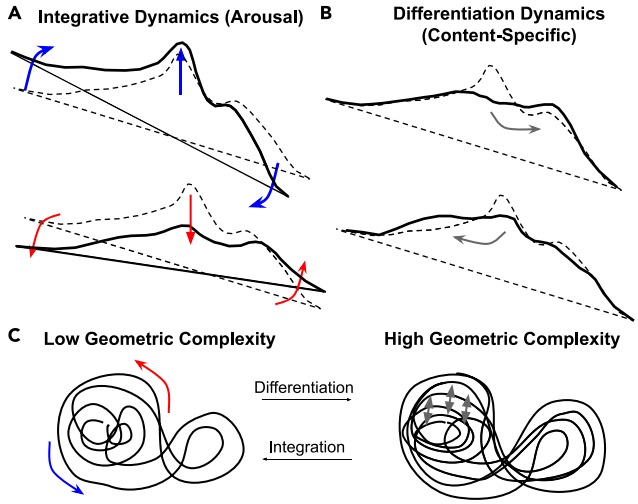

Figure 7. Schematic of spectral features underlying the dynamics of the geometric core

(A) Moment-by-moment fluctuations in arousal underlie integrative core dynamics via changes in the aperiodic slope and the magnitude of alpha power. Top: Decreasing arousal and global inhibition increase the aperiodic slope and alpha power (blue arrows). Bottom: Increasing arousal and global excitation decrease the aperiodic slope and alpha power (red arrows).

(B) Moment-by-moment processing of content-specific, mental-state dynamics arises via differentiation into higher-complexity dynamics. This can occur via shifts toward increased high-frequency power (top) or lower-frequency power (bottom).

(C) Dynamics characterized by low geometric complexity are shared across frequency bands and are therefore capable of integrating global processes and signals (left). Dynamics characterized by high geometric complexity are parameter specific and are therefore more differentiated, capable of representing the richness of mental experience (right).

thalamocortical interactions.[102–104] Given the spatial limitations on EEG generators, we are unable to make a strong claim about underlying anatomy. In fact, it seems likely that our measures reflect large-scale interactions across the brain, such as can occur via non-linear broadcasting.[105] Nonetheless, we speculate that the neurobiology of the geometric core primarily reflects the neurobiology of arousal (including thalamic and brainstem mechanisms), given links between both alpha and aperiodic signals and the arousal process.[47–49,96,106] This perspective also has implications for metabolic constraints on the dynamic core and the energetic cost of signal differentiation and complexity.

Since the brain is incessantly active, the ongoing activity that comprises the dynamic core must also be constrained by energetic cost.[107–110] Energetic constraints are important in models of the dynamics of scale-free neural activity,[111,112] supported by evidence that hypoxia[113] and increased blood glucose flatten the aperiodic slope.[114] Therefore, aperiodic and scale-free dynamics reflect both arousal and metabolic factors, reinforcing a long-established link between states of arousal and metabolism.[115–117] A geometric perspective emphasizes the complexity of arousal,[118–120] whereby heightened arousal is linked to the increased complexity of representational geometry[121] and where energy efficiency corresponds to reduced geometric complexity,[122] as occurs during sleep.[123,124] The complexity of arousal dynamics and diverse topological signatures in neural state space appear to be mediated by burst-like processes in brainstem nuclei,[120,125] consistent with a microgenetic theory of mental process.[39,40] These connections to arousal, energetics, and metabolism suggest that the dynamic core may be concerned with its own dynamical persistence—a concept that Varela referred to as autopoiesis (self-making) and that Deacon has referred to as the "teleodynamic" core of the brain.[126,127] On the basis of the above theoretical and empirical work, we conceptually consider the ongoing dynamics of EEG spectra as "sew-saw," with the fulcrum at the alpha band,[128] and all rhythmic activity emerging from the beam of aperiodic activity (Figure 7A). The dynamics of the aperiodic spectral tilt or rotation reflect states of arousal,[129] with alpha dynamics reflecting whether attention is directed externally or internally and modulated by thalamocortical inhibition.[130,131] Specific frequency-based parameters differentiate out of the more integrative alpha/aperiodic dynamics to yield higher-complexity signals based on the nature or content of the ongoing mental state (Figures 7B and 7C). This proposal sees EEG spectral dynamics as the hallmarks of mental experience, whereby the dynamics of attention and arousal generate an integrative core of activity from which more detailed mental content differentiates. In this manner, we are motivated by a process-developmental theory of mental experience that considers mental states as evolving in form (morphogenesis), more akin to embryology than traditional computation.[39,40]

Loss of complexity in aging

Similar to others, we have found a smaller spectral exponent (shallower slope) in OAs[12] and a reduction in alpha power,[132–134] further supporting the importance of decomposing periodic and aperiodic components for studies of EEG activity in aging.[14] Despite these mean differences in alpha power, we found no differences in alpha complexity between YAs and OAs. By contrast, OAs showed reduced complexity of gamma, beta, and aperiodic complexity. This suggests that the complexity of core dynamics remains largely intact in late life and, in particular, alpha remains a robust predictor of other frequency bands. Nonetheless, the loss of complexity in beta, gamma, and aperiodic parameters occurred concomitantly with an increase in geometric coupling scores between these parameters. We interpret this finding as a loss of high-frequency signal differentiation, that is, the aging brain is more dynamically homogeneous and less complex but more causally efficacious.

This interpretation is consistent with two well-established and related theories of brain aging, namely the loss of complexity in aging and the dedifferentiation hypotheses. The loss of complexity in aging hypothesis proposes that a wide range of physiologic signals show reduction in variability, richness of connectivity, and the degree of hierarchical organization.[51–53] In the aging brain, loss of complexity might result from gray matter and synapse loss, leading to decreased long-range connectivity.[135–137] This process may be related to reduced specificity of regional activation or broadening of tuning curves, generally interpreted as a dedifferentiation in aging.[54–57] Our finding that OA participants showed reduced geometric complexity along with greater geometric coupling is supportive of the signal dedifferentiation hypothesis. This mirrors prior findings of exaggerated alpha-gamma synchronization between nodes of the

default mode network in OAs during the resting state, interpreted as being "stuck" in default mode,[138] or as part of a more robust "redundancy" core.[58] Enhanced synchronization and cross-parameter coupling could reflect compensatory mechanisms to sustain neural dynamics in the face of reduced signal power or complexity.[139–143] Longitudinal studies are needed to determine whether increased synchronization precedes the loss of complexity or results from a compensatory process.

Limitations and future directions

This study has taken a novel geometric approach to analyze the dynamics and cross-parameter coupling of EEG spectral data. We have made use of a publicly available dataset to demonstrate the applicability of this approach to non-clinical human populations and normal aging. A primary limitation of this study is that we have only examined resting-state data. Our approach does not preclude application to task-based experimental design; however, sufficiently long task blocks would be required to capture the EEG spectral manifold and cross-mapping interactions.[144] Nonetheless, that we find differences between EC and EO conditions as well as correlations with the content or resting-state thoughts suggests state dependence of both geometric complexity and cross-parameter coupling. Our application of the dynamic core concept complements fMRI-derived (BOLD) dynamics that are consistent across diverse cognitive tasks[35] by examining dynamics that are consistent across EEG parameters. For task-based applications, one could modify the pipeline we have proposed here to identify principal dimensions of interest based on experimental or task variables or to compare against linear predictions.[73]

Our study is also limited by the fact that the resting-state cognition questionnaire was conducted the day before the EEG session and during an fMRI session. Differences between EEG and fMRI experimental conditions notwithstanding, participants might have had different thought patterns and content during the two sessions. Our analysis was exploratory, so this finding must be interpreted with caution. Nonetheless, it is reasonable to consider that similar thought patterns may persist from day to day.[74–76] Future work will be needed to examine whether such habits of mind can be detected from the geometric shape of brain activity.

Lastly, we have not conducted an exhaustive comparison with information-theoretic approaches that evaluate complexity based on statistical redundancies in the data (e.g., Kolmogorov, Lempel-Ziv, or multiscale entropy).[145,146] Entropy-based approaches have also been applied to infer directed interactions between signals and could be compared to provide an alternative information-theoretic approach to EMCM or CCM.[25–28] In addition, Information-theoretic approaches have not distinguished aperiodic and periodic contributions to the EEG spectra.[147–150] Thus, future work might identify differences between information-theoretic and geometric approaches to EEG spectral data.

We were motivated to explore the geometric structure of EEG data as part of a dynamic core hypothesis and increasing evidence that variability in brain activity can be characterized by dynamic evolution in manifold structure. A rigorous computational comparison of geometric and information-theoretic approaches is outside the scope of the current study. While such a comparison would undoubtedly be informative, it may be equally important to investigate the foundational conceptual and theoretical assumptions that guide the selection of computational models. Our work highlights the need for more data-driven investigations of a process-development model of cognition, whereby mental states evolve from a global, integrative whole to differentiated details.[39,40] Combining a geometric and dynamical systems approach to investigate this model, we might interpret the interactions between neural signals as resemblances among multidimensional shapes in order to characterize the diverse phenomenology of mental experience.[151,152]

EXPERIMENTAL PROCEDURES

Resource availability

Lead contact

Further information and requests for resources should be directed to and will be fulfilled by the lead contact, Dr. Michael Jacob (michael.jacob@ucsf.edu).

Materials availability

This study did not generate new unique materials.

Data and code availability

All of the MATLAB code for the algorithm and analyses in this paper is publicly available online in a Zenodo repository.[153] The EEG and behavioral data utilized is available from the International Neuroimaging Data-sharing Initiative (https://fcon_1000.projects.nitrc.org/indi/retro/MPI_LEMON.html).

EEG dataset

We utilized public-access data from the "Leipzig Study for Mind-Body-Emotion Interactions" (LEMON) dataset that includes 227 healthy participants, including young adult participants (YAs, $N = 153$, mean = 25.1 years, median = 24 years, standard deviation = 3.1, 45 females) and older adult participants (OAs, $N = 74$, mean = 67.6 years, median = 67 years, standard deviation = 4.7, 37 females).[154] Participants in this study underwent a 2-day assessment in Leipzig, Germany between the years 2013 and 2015. The study included resting EEG, fMRI and completion of a battery of neuropsychological and cognitive tests. Participants were free of psychiatric or neurological disorders. For a full list of exclusion criteria, see Babayan et al.[154]

EEG acquisition and preprocessing

Details of the acquisition and preprocessing are available in Babayan et al.[154] The resting-state EEG in the LEMON study was recorded from 216 participants and consisted of 16 resting-state blocks, each lasting 60 s. Half of the blocks were performed with the participant's eyes closed (EC) and the other half with their eyes open (EO). The blocks were visually cued; the participants were seated in front of a computer screen and were instructed to remain awake and focus their gaze on a black cross displayed on a white background during the EO blocks. The recording was done using a BrainAmp MR Plus amplifier, 61 scalp electrodes, and one electrode below the right eye. The EEG data were captured using a band-pass filter with a range of 0.015 Hz to 1 kHz, and the recordings were then converted into a digital format with a sampling rate of 2,500 Hz. After preprocessing, 15 participants were excluded from the analysis due to missing participant demographic information, different sampling rate, and poor data quality (according to Babayan et al.). The raw EEG data were then preprocessed by downsampling to 250 Hz and applying a 1- to 45-Hz band-pass filter. Outlier channels or data intervals were identified by visual inspection and removed. ICA was utilized to reject eye movements, eye blinks, and heartbeats. Here, we utilized the resting-state EEG data from 201 participants (138 YAs and 63 OAs).

EEG processing

The EEG spectra for all channels, participants, and conditions was parameterized into canonical periodic oscillations and aperiodic components using the FOOOF (Fitting Oscillations & One Over F) algorithm (Figure 1B), within a frequency range of 1–45 Hz.[12] We utilized the default parameters for FOOOF, with peak width limits between 1 and 6, peak threshold of 2.0, and "fixed" background mode, which was applied on overlapping, 2-s sliding epochs

with a 0.4-s slide size (80% overlap).[155] The FOOOF algorithm provided good fits for all participants and epochs, with mean R^2 of 0.85 (range 0.76–0.89) for YAs and 0.82 (range 0.72–0.89) for OAs.

The FOOOF fit also yields aperiodic parameters (slope and intercept) and residual periodic power for each epoch, which is determined by subtracting the aperiodic fit from the original spectrum (Figure 1B). We extracted band-pass periodic power within the frequency ranges delta (1–3 Hz), theta (4–7 Hz), alpha (8–12 Hz), beta (15–25 Hz), and low gamma (30–45 Hz), based on the International Federation of Clinical Neurophysiology.[156] For each of the canonical EEG rhythms, an average across a set of channels that contained the highest power was selected for further analysis ({Fz, FC1, FC2, F1, F2, AFz} for delta, theta, and gamma, and {Pz, POz, P1, P2, CP1, CP2, CPz} for alpha and beta). For the aperiodic exponent, an average across a set of channels that contained the shallowest slope was selected for further analysis (F1, F3, FC1, FC3, F2, F4, FC2, FC4).

Comparison of fixed vs. knee aperiodic fit

The complexity of attractor dynamics could be influenced by the nature of the fit from which EEG parameters are derived. In particular, the aperiodic fit can be determined from a bend or "knee" fit rather than a log-linear or "fixed" fit, particularly above 50–75 Hz in intracranial EEG studies.[157,158] Our selection of fit type for EEG parameterization was largely guided by the relatively narrow frequency range under study (1–45 Hz) and prior literature in studies of cognitive aging. Adding a knee parameter did marginally improve the fit in YAs (Figure S1, FIT × AGE $F(1,199) = 30.84$, $p < 0.0001$; yielding a mean improvement in the R^2 value of 0.02, THSD $p < 0.00001$) but did not improve the fit in OAs (yielding a mean reduction in the R^2 value of 0.001, THSD $p = 0.055$, without FIT × AGE × CONDITION effects $F(1,199) = 0.02$, $p = 0.88$). For generalizability and interpretability with existing literature on aging, we selected to further analyze the results for the "fixed" fit.

In the supplemental information, we conducted a methodological validation by examining a "knee" fit for YAs. To ensure that any residual aperiodic activity in the alpha signal was not influencing our measures of geometric complexity, we examined instantaneous and lagged measures of collinearity between EEG parameters before and after the knee fit. Instantaneous collinearity was determined from Pearson's correlation coefficients and lagged correlation from accumulated correlation asymmetry (a measure of temporal precedence between two signals, see supplemental experimental procedures). Reductions in collinearity (Figure S2) and temporal precedence (Figure S3) after knee fit confirmed a linearly purified alpha signal. Nonetheless, after knee fit we found that the alpha attractor remained the least complex relative to all other periodic parameters (Figure S3) and also predicted all other parameters the best (Figure S5). These confirmatory tests suggest that geometric complexity and predictive power are unaffected by whether residual alpha power is determined from a fixed or knee aperiodic fit.

Attractor reconstruction

The overall intuition for our approach combines recent advances in the linear approximation of otherwise non-linear attractor systems based on Koopman theory,[73] with cross-mapping methods to infer causal interactions between attractor manifolds.[23] Based on the assumption that an EEG time series is a projected measurement of higher-dimensional dynamics in the brain,[16] our approach utilizes time-delay embedding to reconstruct the EEG time series in a lower-dimensional state space. This approach is based on Takens' theorem that a smooth attractor can be reconstructed from its one-dimensional measurement such that it is diffeomorphic to the original attractor. Given time series $x(t)$, its embedding in E dimensions can be represented as: $X_E = (x(t), x(t - \tau), x(t - 2\tau), \ldots, x(t - (E - 1)\tau))$, where τ determines how much the original time series is lagged. A τ value of 1 was selected to maximize the noise-smoothing capability of principal component analysis (PCA).[159] The selection of E can be determined directly from the data. Following Tajima et al.,[91] we chose an embedding dimension at which further increases of E would not lead to increases in the CCM score (see below). For the EEG data, we found an average E value of 60 across all participants, parameters, and channels. Random noise (Gaussian with mean zero and standard deviation of 1) was applied to $X_E(t)$ by multiplying a square random matrix from the left in order to reduce autocorrelation and contributions of non-stationarity in the delayed time series (see also Tajima et al.[91]). Other approaches for determining E were considered, such as the false-nearest-neighbor algorithm,[160] but this has been shown to be susceptible to large noisy data.[159]

After finding an appropriate E, we adopt a technique called ETD embedding,[73,161] which applies PCA to $X_E(t)$ and orders the ETD vectors by the fraction of variance they contribute to the original state space, resulting in $V_E = (v_1, v_2, v_3, \ldots, v_E)$, where $X_E v_i = \lambda_i v_i$ for all eigenvectors $v_1, \ldots, v_E$ and eigenvalues $\lambda_1, \ldots \lambda_E$. This approach to data reduction of non-linear methods has been suggested as a way to reduce noise[162] and further construct linear approximations of the system,[73] although this was not further explored in this study. Therefore, our application of PCA to delay embedding yields state space axes that are weighted by their contribution to the overall signal, as has been utilized by others to identify the dynamical core.[35]

Retained components and complexity

In accordance with the Kaiser criterion, we retained all the principal components with eigenvalues above 1, which are the components that captured at least as much variance as a single dimension of the original pre-ETD attractor.[163] Hence, our final reconstructed attractors will be denoted as $V_r = (v_1, v_2, v_3, \ldots, v_r)$, where r represents the number of principal components that are retained. Additionally, we designate r to serve as a measure of geometric complexity, since a larger number of retained components is needed to capture the variance in the data. This approach is intuitively similar to the term topological complexity.[164]

Lyapunov exponent analysis and mean frequency of principal components

We calculated the maximal Lyapunov exponent (MLE) for each ETD-reconstructed dimension to characterize instability (chaotic nature) of their dynamics.[53,165] MATLAB's "lyapunovExponent" function with default parameters was used to measure the MLE for all the retained principal components of ETD-reconstructed attractors.[166] The default variables are the normalized frequency of 2π, embedding dimension of 2, lag of 1, minimum separation time of $\left[\frac{\text{sampling frequency}}{\text{mean frequency}}\right]$, and expansion range of $[1, 5]$. We calculated the mean frequency of our ETD-reconstructed attractors' dimensions to characterize their periodicity using MATLAB's standard "meanfreq" function.

Geometric cross-parameter coupling

We employ a variant of the CCM algorithm to assess shared dynamics and causal influence between two dynamical systems.[23] Briefly, CCM uses the k-nearest-neighbors algorithm in Euclidean space to identify the neighbors for all points in each attractor as well as the weight for each neighbor based on Euclidean distance. The number of neighbors for each point is equal to $r + 1$ (number of dimensions in the attractor, plus 1). For each point in an attractor $V_r(t)$, the set of time indices for its neighbors (arranged in ascending order of distance) and their corresponding weights can be represented as $\{t_1, t_2, \ldots, t_{r+1}\}$ and $\{w_1, w_2, \ldots, w_{r+1}\}$, respectively, where $w_i = \frac{u_i}{\sum u_j}$, for $j = 1, \ldots, r+1$, and $u_i = \exp\left(-\frac{d(V_r(t), V_r(i))}{d(V_r(t), V_r(t_1))}\right)$, where d is the Euclidean distance between the two given points. Subsequently, the algorithm uses the set of neighbors from one attractor to estimate the other and vice versa. For example, we can use attractor $V^1_{r_1}$'s local neighborhood dynamics to estimate attractor $V^2_{r_2}$, where each point in the estimated attractor can be represented as

$$\widehat{V}^2_{r_2}(t) = \sum \left[w_i * V^2_{r_2}(t_i) \right],$$

for $i = 1, \ldots, r_1 + 1$ (see also Figure 4). To obtain a score for the degree of shared dynamics and causality, CCM computes the average of all Pearson correlations between the dimensions of the original manifold and its predicted manifold. We use our eigen modified attractors in CCM to take a weighted average of the correlations across all dimensions based on the eigenvalues from ETD (see the section "attractor reconstruction"). Traditionally, a higher score for the estimation of $\widehat{V}^2$ by V^1 is interpreted as V^2 having a causal influence on V^1: if V^1 obtains a precise estimate of V^2, this can be interpreted as V^1 containing local dynamics about V^2, implying V^2 has previously impacted the dynamics of V^1 by leaving a distinctive geometric imprint.

Statistical approach

To apply both ETD and CCM to examine the dynamics of periodic and aperiodic EEG activity, we utilized the time series of epoched EEG data for delta, theta, alpha, beta, gamma, and the aperiodic exponent (Figure 1B). This yielded six parameter time series of 896 time points (corresponding to 2-s sliding epochs over 6 mins in each condition; see Figure 1C). These time series were subject to both traditional delay embedding and ETD (see Figures 1D and 1E) to determine the complexity for all parameters and all participants. We used repeated-measures ANOVA to examine within-participant effects of CONDITION (EO or EC) and PARAMETER (aperiodic exponent or frequency band) as well as between participant effects of AGE (YA or OA) to examine effects of residual complexity.

We subsequently utilized EMCM and *Z*-scored these values prior to using repeated-measures ANOVA to examine within-participant effects of CONDITION (EO or EC) and PARAMETER (aperiodic exponent or frequency band) as well as between participant effects of AGE (YA or OA) to examine differences in dynamical interactions.

Lastly, we applied factor analysis to the resting-state New York State Cognition Questionnaire. This yielded a distribution of factors matching the results of the original study.[78] We used multiple linear regression to examine relationships between attractor complexity and the form or content of resting-state thinking and corrected for multiple comparisons using the false discovery rate (FDR $p < 0.05$).

SUPPLEMENTAL INFORMATION

Supplemental information can be found online at https://doi.org/10.1016/j.patter.2024.101025.

ACKNOWLEDGMENTS

This work was supported by grants from the Department of Veterans Affairs (IK1CX002089 and IK2CX002457 to M.J.). We gratefully acknowledge the input from our colleagues, who provided valuable comments on an earlier version of the manuscript: Terrence Deacon, Matthew Rogers, Charles Duffy, Adam Jacob, Mani Hamidi, and Judith Ford. We also greatly appreciate the input of two reviewers, Andres Canales-Johnson and an anonymous reviewer, whose feedback significantly improved the manuscript.

AUTHOR CONTRIBUTIONS

Conceptualization, P.P. and M.J.; methodology, P.P. and M.J.; software, P.P.; validation, P.P. and M.J.; formal analysis, P.P. and M.J.; investigation, P.P. and M.J.; data curation, P.P.; writing – original draft, P.P. and M.J.; writing – review & editing, P.P. and M.J.; visualization, P.P. and M.J.; supervision, M.J.; project administration, M.J.; funding acquisition, M.J.

DECLARATION OF INTERESTS

The authors declare no competing interests.

Received: December 6, 2023
Revised: April 28, 2024
Accepted: June 19, 2024
Published: July 19, 2024

REFERENCES

1. Buzsáki, G., and Vöröslakos, M. (2023). Brain rhythms have come of age. Neuron *111*, 922–926.
2. Canolty, R.T., and Knight, R.T. (2010). The functional role of cross-frequency coupling. Trends Cogn. Sci. *14*, 506–515.
3. Hyafil, A., Giraud, A.-L., Fontolan, L., and Gutkin, B. (2015). Neural Cross-Frequency Coupling: Connecting Architectures, Mechanisms, and Functions. Trends Neurosci. *38*, 725–740.
4. Aru, J., Aru, J., Priesemann, V., Wibral, M., Lana, L., Pipa, G., Singer, W., and Vicente, R. (2015). Untangling cross-frequency coupling in neuroscience. Curr. Opin. Neurobiol. *31*, 51–61.
5. Palva, S., and Palva, J.M. (2018). Roles of Brain Criticality and Multiscale Oscillations in Temporal Predictions for Sensorimotor Processing. Trends Neurosci. *41*, 729–743.
6. Mathalon, D.H., and Sohal, V.S. (2015). Neural Oscillations and Synchrony in Brain Dysfunction and Neuropsychiatric Disorders: It's About Time. JAMA Psychiatr. *72*, 840–844.
7. Grover, S., Nguyen, J.A., and Reinhart, R.M.G. (2021). Synchronizing Brain Rhythms to Improve Cognition. Annu. Rev. Med. *72*, 29–43.
8. Florin, E., and Baillet, S. (2015). The brain's resting-state activity is shaped by synchronized cross-frequency coupling of neural oscillations. Neuroimage *111*, 26–35.
9. Marzetti, L., Basti, A., Chella, F., D'Andrea, A., Syrjälä, J., and Pizzella, V. (2019). Brain Functional Connectivity Through Phase Coupling of Neuronal Oscillations: A Perspective From Magnetoencephalography. Front. Neurosci. *13*, 964.
10. Hyafil, A. (2015). Misidentifications of specific forms of cross-frequency coupling: three warnings. Front. Neurosci. *9*, 370.
11. Donoghue, T., Dominguez, J., and Voytek, B. (2020). Electrophysiological Frequency Band Ratio Measures Conflate Periodic and Aperiodic Neural Activity. eNeuro *7*, 10.1523/ENEURO.0192-20.2020. https://doi.org/10.1523/ENEURO.0192-20.2020.
12. Donoghue, T., Haller, M., Peterson, E.J., Varma, P., Sebastian, P., Gao, R., Noto, T., Lara, A.H., Wallis, J.D., Knight, R.T., et al. (2020). Parameterizing neural power spectra into periodic and aperiodic components. Nat. Neurosci. *23*, 1655–1665.
13. Canales-Johnson, A., Teixeira Borges, A.F., Komatsu, M., Fujii, N., Fahrenfort, J.J., Miller, K.J., and Noreika, V. (2021). Broadband Dynamics Rather than Frequency-Specific Rhythms Underlie Prediction Error in the Primate Auditory Cortex. J. Neurosci. *41*, 9374–9391.
14. Tröndle, M., Popov, T., Pedroni, A., Pfeiffer, C., Barańczuk-Turska, Z., and Langer, N. (2023). Decomposing age effects in EEG alpha power. Cortex *161*, 116–144.
15. Breakspear, M. (2017). Dynamic models of large-scale brain activity. Nat. Neurosci. *20*, 340–352.
16. Tozzi, A. (2019). The multidimensional brain. Phys. Life Rev. *31*, 86–103.
17. Stringer, C., Pachitariu, M., Steinmetz, N., Reddy, C.B., Carandini, M., and Harris, K.D. (2019). Spontaneous behaviors drive multidimensional, brainwide activity. Science *364*, 255.
18. Waschke, L., Kloosterman, N.A., Obleser, J., and Garrett, D.D. (2021). Behavior needs neural variability. Neuron *109*, 751–766.
19. Galgali, A.R., Sahani, M., and Mante, V. (2023). Residual dynamics resolves recurrent contributions to neural computation. Nat. Neurosci. *26*, 326–338.
20. Freeman, W.J. (1987). Simulation of chaotic EEG patterns with a dynamic model of the olfactory system. Biol. Cybern. *56*, 139–150.
21. McKenna, T.M., McMullen, T.A., and Shlesinger, M.F. (1994). The brain as a dynamic physical system. Neuroscience *60*, 587–605.
22. Tsuda, I. (2001). Toward an interpretation of dynamic neural activity in terms of chaotic dynamical systems. Behav. Brain Sci. *24*, 793–848. discussion 810–848.
23. Sugihara, G., May, R., Ye, H., Hsieh, C.-H., Deyle, E., Fogarty, M., and Munch, S. (2012). Detecting causality in complex ecosystems. Science *338*, 496–500.
24. Ye, H., Beamish, R.J., Glaser, S.M., Grant, S.C.H., Hsieh, C.-H., Richards, L.J., Schnute, J.T., and Sugihara, G. (2015). Equation-free mechanistic ecosystem forecasting using empirical dynamic modeling. Proc. Natl. Acad. Sci. USA *112*, E1569–E1576.
25. Imperatori, L.S., Betta, M., Cecchetti, L., Canales-Johnson, A., Ricciardi, E., Siclari, F., Pietrini, P., Chennu, S., and Bernardi, G. (2019). EEG functional connectivity metrics wPLI and wSMI account for distinct types of brain functional interactions. Sci. Rep. *9*, 8894.

26. Canales-Johnson, A., Beerendonk, L., Chennu, S., Davidson, M.J., Ince, R.A.A., and van Gaal, S. (2023). Feedback information transfer in the human brain reflects bistable perception in the absence of report. PLoS Biol. *21*, e3002120.

27. King, J.-R., Sitt, J.D., Faugeras, F., Rohaut, B., El Karoui, I., Cohen, L., Naccache, L., and Dehaene, S. (2013). Information sharing in the brain indexes consciousness in noncommunicative patients. Curr. Biol. *23*, 1914–1919.

28. Canales-Johnson, A., Billig, A.J., Olivares, F., Gonzalez, A., Garcia, M.D.C., Silva, W., Vaucheret, E., Ciraolo, C., Mikulan, E., Ibanez, A., et al. (2020). Corrigendum: Dissociable Neural Information Dynamics of Perceptual Integration and Differentiation during Bistable Perception. Cereb. Cortex *30*, 3856.

29. James, R.G., Barnett, N., and Crutchfield, J.P. (2016). Information Flows? A Critique of Transfer Entropies. Phys. Rev. Lett. *116*, 238701.

30. Deng, J., Sun, B., Scheel, N., Renli, A.B., Zhu, D.C., Zhu, D., Ren, J., Li, T., and Zhang, R. (2024). Causalized convergent cross-mapping and its approximate equivalence with directed information in causality analysis. PNAS Nexus *3*, gad422.

31. Schiecke, K., Schumann, A., Benninger, F., Feucht, M., Baer, K.-J., and Schlattmann, P. (2019). Brain-heart interactions considering complex physiological data: processing schemes for time-variant, frequency-dependent, topographical and statistical examination of directed interactions by convergent cross mapping. Physiol. Meas. *40*, 114001.

32. Chung, S., and Abbott, L.F. (2021). Neural population geometry: An approach for understanding biological and artificial neural networks. Curr. Opin. Neurobiol. *70*, 137–144.

33. Azeredo da Silveira, R., and Rieke, F. (2021). The geometry of information coding in correlated neural populations. Annu. Rev. Neurosci. *44*, 403–424.

34. Kriegeskorte, N., and Wei, X.-X. (2021). Neural tuning and representational geometry. Nat. Rev. Neurosci. *22*, 703–718.

35. Shine, J.M., Breakspear, M., Bell, P.T., Ehgoetz Martens, K.A., Shine, R., Koyejo, O., Sporns, O., and Poldrack, R.A. (2019). Human cognition involves the dynamic integration of neural activity and neuromodulatory systems. Nat. Neurosci. *22*, 289–296.

36. Varela, F.J. (1995). Resonant cell assemblies: a new approach to cognitive functions and neuronal synchrony. Biol. Res. *28*, 81–95.

37. Le Van Quyen, M. (2003). Disentangling the dynamic core: a research program for a neurodynamics at the large-scale. Biol. Res. *36*, 67–88.

38. Varela, F. (1979). Principles of Biological Autonomy.

39. Brown, J.W. (2013). Introduction: microgenetic theory. In The life of the mind (Psychology Press), pp. 1–26.

40. Deacon, T. (1989). Holism and associationism in neuropsychology: An anatomical synthesis. In Integrating Theory and Practice in Clinical Neuropsychology, E. Perecman, ed. (Routledge), pp. 1–48.

41. Jacob, P. (1954). The Behavior Cycle: An Interpretation of Behavior from the Standpoint of an Educationist (Edwards Brothers).

42. Tononi, G., and Edelman, G.M. (1998). Consciousness and complexity. Science *282*, 1846–1851.

43. Mölle, M., Marshall, L., Wolf, B., Fehm, H.L., and Born, J. (1999). EEG complexity and performance measures of creative thinking. Psychophysiology *36*, 95–104.

44. Lutzenberger, W., Elbert, T., Birbaumer, N., Ray, W.J., and Schupp, H. (1992). The scalp distribution of the fractal dimension of the EEG and its variation with mental tasks. Brain Topogr. *5*, 27–34.

45. Merker, B., Williford, K., and Rudrauf, D. (2021). The integrated information theory of consciousness: A case of mistaken identity. Behav. Brain Sci. *45*, e41.

46. Mediano, P.A.M., Rosas, F.E., Bor, D., Seth, A.K., and Barrett, A.B. (2022). The strength of weak integrated information theory. Trends Cogn. Sci. *26*, 646–655.

47. Colombo, M.A., Napolitani, M., Boly, M., Gosseries, O., Casarotto, S., Rosanova, M., Brichant, J.-F., Boveroux, P., Rex, S., Laureys, S., et al. (2019). The spectral exponent of the resting EEG indexes the presence of consciousness during unresponsiveness induced by propofol, xenon, and ketamine. Neuroimage *189*, 631–644.

48. Lendner, J.D., Helfrich, R.F., Mander, B.A., Romundstad, L., Lin, J.J., Walker, M.P., Larsson, P.G., and Knight, R.T. (2020). An electrophysiological marker of arousal level in humans. Elife *9*, e55092. https://doi.org/10.7554/eLife.55092.

49. Medel, V., Irani, M., Crossley, N., Ossandón, T., and Boncompte, G. (2023). Complexity and 1/f slope jointly reflect brain states. Sci. Rep. *13*, 21700.

50. Sorscher, B., Ganguli, S., and Sompolinsky, H. (2022). Neural representational geometry underlies few-shot concept learning. Proc. Natl. Acad. Sci. USA *119*, e2200800119.

51. Lipsitz, L.A., and Goldberger, A.L. (1992). Loss of "Complexity" and Aging: Potential Applications of Fractals and Chaos Theory to Senescence. JAMA *267*, 1806–1809.

52. Vaillancourt, D.E., and Newell, K.M. (2002). Changing complexity in human behavior and physiology through aging and disease. Neurobiol. Aging *23*, 1–11.

53. Ma, M.K.-H., Fong, M.C.-M., Xie, C., Lee, T., Chen, G., and Wang, W.S. (2021). Regularity and randomness in ageing: Differences in resting-state EEG complexity measured by largest Lyapunov exponent. Neuroimage: Reports *1*, 100054.

54. Park, D.C., Polk, T.A., Park, R., Minear, M., Savage, A., and Smith, M.R. (2004). Aging reduces neural specialization in ventral visual cortex. Proc. Natl. Acad. Sci. USA *101*, 13091–13095.

55. Heuninckx, S., Wenderoth, N., and Swinnen, S.P. (2008). Systems neuroplasticity in the aging brain: recruiting additional neural resources for successful motor performance in elderly persons. J. Neurosci. *28*, 91–99.

56. Sleimen-Malkoun, R., Temprado, J.-J., and Hong, S.L. (2014). Aging induced loss of complexity and dedifferentiation: consequences for coordination dynamics within and between brain, muscular and behavioral levels. Front. Aging Neurosci. *6*, 140.

57. Rakesh, D., Fernando, K.B., and Mansour L, S. (2020). Functional dedifferentiation of the brain during healthy aging. J. Neurophysiol. *123*, 1279–1282.

58. Gatica, M., Cofré, R., Mediano, P.A.M., Rosas, F.E., Orio, P., Diez, I., Swinnen, S.P., and Cortes, J.M. (2021). High-Order Interdependencies in the Aging Brain. Brain Connect. *11*, 734–744.

59. Finley, A.J., Angus, D.J., van Reekum, C.M., Davidson, R.J., and Schaefer, S.M. (2022). Periodic and aperiodic contributions to theta-beta ratios across adulthood. Psychophysiology *59*, e14113.

60. Merkin, A., Sghirripa, S., Graetz, L., Smith, A.E., Hordacre, B., Harris, R., Pitcher, J., Semmler, J., Rogasch, N.C., and Goldsworthy, M. (2023). Do age-related differences in aperiodic neural activity explain differences in resting EEG alpha? Neurobiol. Aging *121*, 78–87.

61. Finley, A.J., Angus, D.J., Knight, E.L., van Reekum, C.M., Lachman, M.E., Davidson, R.J., and Schaefer, S.M. (2024). Resting EEG Periodic and Aperiodic Components Predict Cognitive Decline Over 10 Years. J. Neurosci. *44*, e1332232024. https://doi.org/10.1523/JNEUROSCI.1332-23.2024.

62. Voytek, B., Kramer, M.A., Case, J., Lepage, K.Q., Tempesta, Z.R., Knight, R.T., and Gazzaley, A. (2015). Age-Related Changes in 1/f Neural Electrophysiological Noise. J. Neurosci. *35*, 13257–13265.

63. Palva, J.M., Zhigalov, A., Hirvonen, J., Korhonen, O., Linkenkaer-Hansen, K., and Palva, S. (2013). Neuronal long-range temporal correlations and avalanche dynamics are correlated with behavioral scaling laws. Proc. Natl. Acad. Sci. USA *110*, 3585–3590.

64. Poil, S.-S., Hardstone, R., Mansvelder, H.D., and Linkenkaer-Hansen, K. (2012). Critical-state dynamics of avalanches and oscillations jointly emerge from balanced excitation/inhibition in neuronal networks. J. Neurosci. *32*, 9817–9823.

65. Brake, N., Duc, F., Rokos, A., Arseneau, F., Shahiri, S., Khadra, A., and Plourde, G. (2024). A neurophysiological basis for aperiodic EEG and the background spectral trend. Nat. Commun. *15*, 1514.

66. Gao, R., Peterson, E.J., and Voytek, B. (2017). Inferring synaptic excitation/inhibition balance from field potentials. Neuroimage *158*, 70–78.

67. Nanda, A., Johnson, G.W., Mu, Y., Ahrens, M.B., Chang, C., Englot, D.J., Breakspear, M., and Rubinov, M. (2023). Time-resolved correlation of distributed brain activity tracks E-I balance and accounts for diverse scale-free phenomena. Cell Rep. *42*, 112254.

68. Palva, J.M., and Palva, S. (2014). The correlation of the neuronal long-range temporal correlations, avalanche dynamics with the behavioral scaling laws and interindividual variability. In Criticality in Neural Systems (Wiley-VCH Verlag GmbH & Co. KGaA), pp. 105–126.

69. Fuscà, M., Siebenhühner, F., Wang, S.H., Myrov, V., Arnulfo, G., Nobili, L., Palva, J.M., and Palva, S. (2023). Brain criticality predicts individual levels of inter-areal synchronization in human electrophysiological data. Nat. Commun. *14*, 4736.

70. He, B.J., Zempel, J.M., Snyder, A.Z., and Raichle, M.E. (2010). The temporal structures and functional significance of scale-free brain activity. Neuron *66*, 353–369.

71. Pei, L., Zhou, X., Leung, F.K.S., and Ouyang, G. (2023). Differential associations between scale-free neural dynamics and different levels of cognitive ability. Psychophysiology *60*, e14259.

72. Pani, S.M., Saba, L., and Fraschini, M. (2022). Clinical applications of EEG power spectra aperiodic component analysis: A mini-review. Clin. Neurophysiol. *143*, 1–13.

73. Brunton, S.L., Brunton, B.W., Proctor, J.L., Kaiser, E., and Kutz, J.N. (2017). Chaos as an intermittently forced linear system. Nat. Commun. *8*, 19.

74. Hertel, P.T. (2004). Habits of thought produce memory biases in anxiety and depression. In Cognition, Emotion and Psychopathology: Theoretical, Empirical and Clinical Directions, J. Yiend, ed., pp. 109–129.

75. Watkins, E.R., and Nolen-Hoeksema, S. (2014). A habit-goal framework of depressive rumination. J. Abnorm. Psychol. *123*, 24–34.

76. Colvin, E., Gardner, B., Labelle, P.R., and Santor, D. (2021). The automaticity of positive and negative thinking: A scoping review of mental habits. Cognit. Ther. Res. *45*, 1037–1063.

77. Adams, R.A., Vincent, P., Benrimoh, D., Friston, K.J., and Parr, T. (2022). Everything is connected: Inference and attractors in delusions. Schizophr. Res. *245*, 5–22.

78. Gorgolewski, K.J., Lurie, D., Urchs, S., Kipping, J.A., Craddock, R.C., Milham, M.P., Margulies, D.S., and Smallwood, J. (2014). A correspondence between individual differences in the brain's intrinsic functional architecture and the content and form of self-generated thoughts. PLoS One *9*, e97176.

79. Rudrauf, D., Lutz, A., Cosmelli, D., Lachaux, J.-P., and Le Van Quyen, M. (2003). From autopoiesis to neurophenomenology: Francisco Varela's exploration of the biophysics of being. Biol. Res. *36*, 27–65.

80. Kwessi, E.A., and Edwards, L.J. (2021). Analysis of EEG Data Using Complex Geometric Structurization. Neural Comput. *33*, 1942–1969.

81. Akbari, H., Sadiq, M.T., Ur Rehman, A., Ghazvini, M., Naqvi, R.A., Payan, M., Bagheri, H., and Bagheri, H. (2021). Depression recognition based on the reconstruction of phase space of EEG signals and geometrical features. Appl. Acoust. *179*, 108078.

82. Varley, T.F., Denny, V., Sporns, O., and Patania, A. (2021). Topological analysis of differential effects of ketamine and propofol anaesthesia on brain dynamics. R. Soc. Open Sci. *8*, 201971.

83. Kilner, J.M., Mattout, J., Henson, R., and Friston, K.J. (2005). Hemodynamic correlates of EEG: a heuristic. Neuroimage *28*, 280–286.

84. Fries, P., Scheeringa, R., and Oostenveld, R. (2008). Finding gamma. Neuron *58*, 303–305.

85. Herrmann, C.S., Fründ, I., and Lenz, D. (2010). Human gamma-band activity: a review on cognitive and behavioral correlates and network models. Neurosci. Biobehav. Rev. *34*, 981–992.

86. White, R.S., and Siegel, S.J. (2016). Cellular and circuit models of increased resting-state network gamma activity in schizophrenia. Neuroscience *321*, 66–76.

87. Wang, J., Liu, Q., Tian, F., Zhou, S., Parra, M.A., Wang, H., and Yu, X. (2022). Disrupted Spatiotemporal Complexity of Resting-State Electroencephalogram Dynamics Is Associated With Adaptive and Maladaptive Rumination in Major Depressive Disorder. Front. Neurosci. *16*, 829755.

88. Diaz, B.A., Van Der Sluis, S., Moens, S., Benjamins, J.S., Migliorati, F., Stoffers, D., Den Braber, A., Poil, S.-S., Hardstone, R., Van't Ent, D., et al. (2013). The Amsterdam Resting-State Questionnaire reveals multiple phenotypes of resting-state cognition. Front. Hum. Neurosci. *7*, 446.

89. Lomas, T., Ivtzan, I., and Fu, C.H.Y. (2015). A systematic review of the neurophysiology of mindfulness on EEG oscillations. Neurosci. Biobehav. Rev. *57*, 401–410.

90. Engel, A.K., Gerloff, C., Hilgetag, C.C., and Nolte, G. (2013). Intrinsic coupling modes: multiscale interactions in ongoing brain activity. Neuron *80*, 867–886.

91. Tajima, S., Yanagawa, T., Fujii, N., and Toyoizumi, T. (2015). Untangling Brain-Wide Dynamics in Consciousness by Cross-Embedding. PLoS Comput. Biol. *11*, e1004537.

92. Cocina, F., Vitalis, A., and Caflisch, A. (2021). Unsupervised Methods for Detection of Neural States: Case Study of Hippocampal-Amygdala Interactions. eNeuro *8*, 10.1523/ENEURO.0484-20.2021. https://doi.org/10.1523/ENEURO.0484-20.2021.

93. McBride, J.C., Zhao, X., Munro, N.B., Jicha, G.A., Schmitt, F.A., Kryscio, R.J., Smith, C.D., and Jiang, Y. (2015). Sugihara causality analysis of scalp EEG for detection of early Alzheimer's disease. Neuroimage. Clin. *7*, 258–265.

94. Fonseca, A., Kerick, S., King, J.-T., Lin, C.-T., and Jung, T.-P. (2018). Brain Network Changes in Fatigued Drivers: A Longitudinal Study in a Real-World Environment Based on the Effective Connectivity Analysis and Actigraphy Data. Front. Hum. Neurosci. *12*, 418.

95. Lainscsek, C., Gonzalez, C.E., Sampson, A.L., Cash, S.S., and Sejnowski, T.J. (2019). Causality detection in cortical seizure dynamics using cross-dynamical delay differential analysis. Chaos *29*, 101103.

96. Ota, T., Toyoshima, R., and Yamauchi, T. (1996). Measurements by biphasic changes of the alpha band amplitude as indicators of arousal level. Int. J. Psychophysiol. *24*, 25–37.

97. Colombo, M.A., Comanducci, A., Casarotto, S., Derchi, C.-C., Annen, J., Viganò, A., Mazza, A., Trimarchi, P.D., Boly, M., Fecchio, M., et al. (2023). Beyond alpha power: EEG spatial and spectral gradients robustly stratify disorders of consciousness. Cereb. Cortex *33*, 7193–7210.

98. Jacob, M.S., Roach, B.J., Sargent, K.S., Mathalon, D.H., and Ford, J.M. (2021). Aperiodic measures of neural excitability are associated with anticorrelated hemodynamic networks at rest: A combined EEG-fMRI study. Neuroimage *245*, 118705.

99. Jensen, O., and Mazaheri, A. (2010). Shaping functional architecture by oscillatory alpha activity: gating by inhibition. Front. Hum. Neurosci. *4*, 186.

100. Min, B.-K., Kim, H.S., Pinotsis, D.A., and Pantazis, D. (2020). Thalamocortical inhibitory dynamics support conscious perception. Neuroimage *220*, 117066.

101. Ward, L.M. (2011). The thalamic dynamic core theory of conscious experience. Conscious. Cogn. *20*, 464–486.

102. Lopes da Silva, F.H., Hoeks, A., Smits, H., and Zetterberg, L.H. (1974). Model of brain rhythmic activity. The alpha-rhythm of the thalamus. Kybernetik *15*, 27–37.

103. Halgren, M., Ulbert, I., Bastuji, H., Fabó, D., Erőss, L., Rey, M., Devinsky, O., Doyle, W.K., Mak-McCully, R., Halgren, E., et al. (2019). The generation and propagation of the human alpha rhythm. Proc. Natl. Acad. Sci. USA *116*, 23772–23782.

104. de Munck, J.C., Gonçalves, S.I., Huijboom, L., Kuijer, J.P.A., Pouwels, P.J.W., Heethaar, R.M., and Lopes da Silva, F.H. (2007). The

hemodynamic response of the alpha rhythm: an EEG/fMRI study. Neuroimage *35*, 1142–1151.

105. Vinck, M., Uran, C., Spyropoulos, G., Onorato, I., Broggini, A.C., Schneider, M., and Canales-Johnson, A. (2023). Principles of large-scale neural interactions. Neuron *111*, 987–1002.
106. Johnston, R., Snyder, A.C., Schibler, R.S., and Smith, M.A. (2022). EEG Signals Index a Global Signature of Arousal Embedded in Neuronal Population Recordings. eNeuro *9*, 10.1523/ENEURO.0012-22.2022. https://doi.org/10.1523/ENEURO.0012-22.2022.
107. Raichle, M.E., and Gusnard, D.A. (2002). Appraising the brain's energy budget. Proc. Natl. Acad. Sci. USA *99*, 10237–10239.
108. Howarth, C., Gleeson, P., and Attwell, D. (2012). Updated energy budgets for neural computation in the neocortex and cerebellum. J. Cereb. Blood Flow Metab. *32*, 1222–1232.
109. Christie, S.T., and Schrater, P. (2015). Cognitive cost as dynamic allocation of energetic resources. Front. Neurosci. *9*, 289.
110. Levy, W.B., and Calvert, V.G. (2021). Communication consumes 35 times more energy than computation in the human cortex, but both costs are needed to predict synapse number. Proc. Natl. Acad. Sci. USA *118*, e2008173118. https://doi.org/10.1073/pnas.2008173118.
111. Roberts, J.A., Iyer, K.K., Vanhatalo, S., and Breakspear, M. (2014). Critical role for resource constraints in neural models. Front. Syst. Neurosci. *8*, 154.
112. Burroni, J., Taylor, P., Corey, C., Vachnadze, T., and Siegelmann, H.T. (2017). Energetic Constraints Produce Self-sustained Oscillatory Dynamics in Neuronal Networks. Front. Neurosci. *11*, 80.
113. Coronel-Oliveros, C., Medel, V., Whitaker, G.A., Astudillo, A., Gallagher, D., Z-Rivera, L., Prado, P., El-Deredy, W., Orio, P., and Weinstein, A. (2024). Elevating understanding: Linking high-altitude hypoxia to brain aging through EEG functional connectivity and spectral analyses. Netw. Neurosci. *8*, 275–292.
114. Walker, C.P., Buse, J.B., and Frohlich, F. (2021). Experimental increase of blood glucose alters resting state EEG measures of excitation-inhibition balance. Exp. Physiol. *106*, 803–811.
115. Mattson, M.P., Moehl, K., Ghena, N., Schmaedick, M., and Cheng, A. (2018). Intermittent metabolic switching, neuroplasticity and brain health. Nat. Rev. Neurosci. *19*, 63–80.
116. Anafi, R.C., Kayser, M.S., and Raizen, D.M. (2019). Exploring phylogeny to find the function of sleep. Nat. Rev. Neurosci. *20*, 109–116.
117. Siegel, J.M. (2022). Sleep function: an evolutionary perspective. Lancet Neurol. *21*, 937–946.
118. Thayer, R.E. (1978). Toward a psychological theory of multidimensional activation (arousal). Motiv. Emot. *2*, 1–34.
119. Trofimova, I., and Robbins, T.W. (2016). Temperament and arousal systems: A new synthesis of differential psychology and functional neurochemistry. Neurosci. Biobehav. Rev. *64*, 382–402.
120. Munn, B.R., Müller, E.J., Wainstein, G., and Shine, J.M. (2021). The ascending arousal system shapes neural dynamics to mediate awareness of cognitive states. Nat. Commun. *12*, 6016.
121. Fekete, T., Pitowsky, I., Grinvald, A., and Omer, D.B. (2009). Arousal increases the representational capacity of cortical tissue. J. Comput. Neurosci. *27*, 211–227.
122. Tozzi, A., and Peters, J.F. (2017). From abstract topology to real thermodynamic brain activity. Cogn. Neurodyn. *11*, 283–292.
123. Jeong, J., Kim, D.J., Kim, S.Y., Chae, J.H., Go, H.J., and Kim, K.S. (2001). Effect of total sleep deprivation on the dimensional complexity of the waking EEG. Sleep *24*, 197–202.
124. Röschke, J., and Aldenhoff, J. (1991). The dimensionality of human's electroencephalogram during sleep. Biol. Cybern. *64*, 307–313.
125. Munn, B.R., Müller, E.J., Medel, V., Naismith, S.L., Lizier, J.T., Sanders, R.D., and Shine, J.M. (2023). Neuronal connected burst cascades bridge macroscale adaptive signatures across arousal states. Nat. Commun. *14*, 1–17.
126. Deacon, T.W. (2011). Incomplete Nature: How Mind Emerged from Matter (WW Norton & Company).
127. Jacob, M., Ford, J., and Deacon, T. (2023). Cognition is entangled with metabolism: relevance for resting-state EEG-fMRI. Front. Hum. Neurosci. *17*, 976036.
128. Garcia-Rill, E., D'Onofrio, S., Luster, B., Mahaffey, S., Urbano, F.J., and Phillips, C. (2016). The 10 Hz frequency: A fulcrum for transitional brain states. Transl. Brain Rhythm. *1*, 7–13.
129. Podvalny, E., Noy, N., Harel, M., Bickel, S., Chechik, G., Schroeder, C.E., Mehta, A.D., Tsodyks, M., and Malach, R. (2015). A unifying principle underlying the extracellular field potential spectral responses in the human cortex. J. Neurophysiol. *114*, 505–519.
130. Knyazev, G.G., Savostyanov, A.N., Bocharov, A.V., Dorosheva, E.A., Tamozhnikov, S.S., and Saprigyn, A.E. (2015). Oscillatory correlates of autobiographical memory. Int. J. Psychophysiol. *95*, 322–332.
131. Knyazev, G.G., Savostyanov, A.N., Volf, N.V., Liou, M., and Bocharov, A.V. (2012). EEG correlates of spontaneous self-referential thoughts: a cross-cultural study. Int. J. Psychophysiol. *86*, 173–181.
132. Roubicek, J. (1977). The electroencephalogram in the middle-aged and the elderly. J. Am. Geriatr. Soc. *25*, 145–152.
133. Breslau, J., Starr, A., Sicotte, N., Higa, J., and Buchsbaum, M.S. (1989). Topographic EEG changes with normal aging and SDAT. Electroencephalogr. Clin. Neurophysiol. *72*, 281–289.
134. Vysata, O., Kukal, J., Prochazka, A., Pazdera, L., and Valis, M. (2012). Age-Related Changes in the Energy and Spectral Composition of EEG. Neurophysiology *44*, 63–67.
135. Huttenlocher, P.R. (1979). Synaptic density in human frontal cortex - developmental changes and effects of aging. Brain Res. *163*, 195–205.
136. Masliah, E., Mallory, M., Hansen, L., DeTeresa, R., and Terry, R.D. (1993). Quantitative synaptic alterations in the human neocortex during normal aging. Neurology *43*, 192–197.
137. Scheff, S.W., and Price, D.A. (2003). Synaptic pathology in Alzheimer's disease: a review of ultrastructural studies. Neurobiol. Aging *24*, 1029–1046.
138. Pinal, D., Zurrón, M., Díaz, F., and Sauseng, P. (2015). Stuck in default mode: inefficient cross-frequency synchronization may lead to age-related short-term memory decline. Neurobiol. Aging *36*, 1611–1618.
139. Ansado, J., Monchi, O., Ennabil, N., Faure, S., and Joanette, Y. (2012). Load-dependent posterior–anterior shift in aging in complex visual selective attention situations. Brain Res. *1454*, 14–22.
140. Meunier, D., Stamatakis, E.A., and Tyler, L.K. (2014). Age-related functional reorganization, structural changes, and preserved cognition. Neurobiol. Aging *35*, 42–54.
141. Jacob, M.S., and Duffy, C.J. (2014). Might cortical hyper-responsiveness in aging contribute to Alzheimer's disease? PLoS One *9*, e105962.
142. Morcom, A.M., and Henson, R.N.A. (2018). Increased Prefrontal Activity with Aging Reflects Nonspecific Neural Responses Rather than Compensation. J. Neurosci. *38*, 7303–7313.
143. Zahodne, L.B., and Reuter-Lorenz, P.A. (2019). Compensation and brain aging: A review and analysis of evidence. In The Aging Brain: Functional Adaptation Across Adulthood, G.R. Samanez-Larkin, ed. (American Psychological Association), pp. 185–216.
144. Maher, M.C., and Hernandez, R.D. (2015). CauseMap: fast inference of causality from complex time series. PeerJ *3*, e824.
145. Wang, J. (2012). Geometric Structure of High-Dimensional Data and Dimensionality Reduction (Springer).
146. Cafaro, C., and Ali, S.A. (2021). Information Geometric Measures of Complexity with Applications to Classical and Quantum Physical Settings. Foundations *1*, 45–62.
147. González, J., Mateos, D., Cavelli, M., Mondino, A., Pascovich, C., Torterolo, P., and Rubido, N. (2022). Low frequency oscillations drive EEG's complexity changes during wakefulness and sleep. Neuroscience *494*, 1–11.

148. Al-Nuaimi, A.H.H., Jammeh, E., Sun, L., and Ifeachor, E. (2018). Complexity Measures for Quantifying Changes in Electroencephalogram in Alzheimer's Disease. Complexity *2018*, 1–12. https://doi.org/10.1155/2018/8915079.

149. Pappalettera, C., Cacciotti, A., Nucci, L., Miraglia, F., Rossini, P.M., and Vecchio, F. (2023). Approximate entropy analysis across electroencephalographic rhythmic frequency bands during physiological aging of human brain. Geroscience *45*, 1131–1145.

150. Sun, J., Wang, B., Niu, Y., Tan, Y., Fan, C., Zhang, N., Xue, J., Wei, J., and Xiang, J. (2020). Complexity Analysis of EEG, MEG, and fMRI in Mild Cognitive Impairment and Alzheimer's Disease: A Review. Entropy *22*, 239. https://doi.org/10.3390/e22020239.

151. Williams, D., and Colling, L. (2018). From symbols to icons: the return of resemblance in the cognitive neuroscience revolution. Synthese *195*, 1941–1967.

152. Deacon, T.W. (2022). Steps to a semiotic cognitive neuroscience. In The Routledge Handbook of Semiosis and the Brain, A.M. García and A. Ibáñez, eds. (Taylor & Francis).

153. Pourdavood, P. (2024). Eigen Manifold Cross Mapping Toolbox. Zenodo. https://doi.org/10.5281/zenodo.11062690.

154. Babayan, A., Erbey, M., Kumral, D., Reinelt, J.D., Reiter, A.M.F., Röbbig, J., Schaare, H.L., Uhlig, M., Anwander, A., Bazin, P.-L., et al. (2019). A mind-brain-body dataset of MRI, EEG, cognition, emotion, and peripheral physiology in young and old adults. Sci. Data *6*, 180308.

155. Al-Salman, W., Li, Y., and Wen, P. (2019). K-complexes Detection in EEG Signals using Fractal and Frequency Features Coupled with an Ensemble Classification Model. Neuroscience *422*, 119–133.

156. Babiloni, C., Barry, R.J., Başar, E., Blinowska, K.J., Cichocki, A., Drinkenburg, W.H.I.M., Klimesch, W., Knight, R.T., Lopes da Silva, F., Nunez, P., et al. (2020). International Federation of Clinical Neurophysiology (IFCN) - EEG research workgroup: Recommendations on frequency and topographic analysis of resting state EEG rhythms. Part 1: Applications in clinical research studies. Clin. Neurophysiol. *131*, 285–307.

157. Gerster, M., Waterstraat, G., Litvak, V., Lehnertz, K., Schnitzler, A., Florin, E., Curio, G., and Nikulin, V. (2022). Separating Neural Oscillations from Aperiodic 1/f Activity: Challenges and Recommendations. Neuroinformatics *20*, 991–1012.

158. He, B.J. (2014). Scale-free brain activity: past, present, and future. Trends Cogn. Sci. *18*, 480–487.

159. Rhodes, C., and Morari, M. (1997). False-nearest-neighbors algorithm and noise-corrupted time series. Phys. Rev. E *55*, 6162–6170.

160. Kennel, M.B., Brown, R., and Abarbanel, H.D. (1992). Determining embedding dimension for phase-space reconstruction using a geometrical construction. Phys. Rev. A *45*, 3403–3411.

161. Juang, J.-N., and Pappa, R.S. (1985). An eigensystem realization algorithm for modal parameter identification and model reduction. J. Guid. Control Dyn. *8*, 620–627.

162. Hegger, R., Kantz, H., and Schreiber, T. (1999). Practical implementation of nonlinear time series methods: The TISEAN package. Chaos *9*, 413–435.

163. Kaiser, H.F. (1960). The Application of Electronic Computers to Factor Analysis. Educ. Psychol. Meas. *20*, 141–151.

164. Moyal, R., and Edelman, S. (2019). Dynamic Computation in Visual Thalamocortical Networks. Entropy *21*, 500. https://doi.org/10.3390/e21050500.

165. Miller, R.H. (1964). Irreversibility in Small Stellar Dynamical Systems. Astrophys. J. *140*, 250.

166. Rosenstein, M.T., Collins, J.J., and De Luca, C.J. (1993). A practical method for calculating largest Lyapunov exponents from small data sets. Physica D *65*, 117–134.